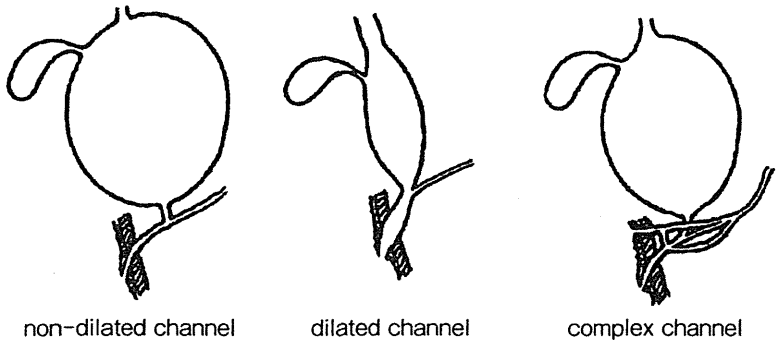

図 2 戸谷らの分類（文献 13 より引用改変）

⑧戸谷らの分類[13]（図 2）

共通管や副膵管の拡張例に蛋白栓や膵石，膵炎が多いことから，共通管に拡張がない non-dilated channel，拡張のある dilated channel，複雑な complex channel との 3 型に分類している。

共通管非拡張型 non-dilated channel：Ⅰaや Ⅳ-A 型の嚢胞状拡張に多くみられるが，紡錘または円筒状拡張例にもみられる。

共通管拡張型 dilated channel：共通管に拡張があり，Ⅰc 型など胆管拡張が大きくないものに多く，蛋白栓，膵石，膵炎などをしばしば合併する。

複雑型 complex channel：複雑な合流形態を示すもので，膵病変をしばしば合併する。膵管癒合不全も包含する。

最近，戸谷はこれら 3 型に共通管が長くて合流異常とよく似た病態を示す不全型（膵胆管高位合流型）abortive type を追加している[14]。

Ⅱ．型分類に関する考察

1．発生学の面から

合流異常の発生原因は十分には解明されておらず，膵・胆管の発生をもとに推論するしかない。これまで理解されている膵・胆管の発生学によると，膵原基は左右 2 葉からなる腹側膵原基と背側膵原基からなり，総胆管を形成する肝憩室と腹側膵原基は左右腹側膵原基の 2 本の導管でつながり癒合している（図 3a）。その後，左腹側膵原基は退化し，右腹側膵原基が十二指腸を軸に時計方向に 180° 回転し，胎生 6 週ごろに背側膵原基の背側に達し癒合するとされている[15,16]。したがって多くの研究者は合流異常は腹側膵管と胆管の発生異常が原因と考えており，嚢胞状拡張などでみられる胆管末端狭小部は腹側膵管由来で，左腹側膵管の遺残あるいは腹側膵管の分枝で，本来存在すべき総胆管末端部が消失した結果，胆管が左腹側膵管あるいは腹側膵管の分枝と交通したものとされている[16~18]。一方，右腹側膵管が消失した場合にはあまり拡張のない合流異常が発生する（図 3）。著者自身はこれらの説が最も説得力があり，狭窄部の存在が胆管拡張の重要な因子であることにはまず間違いないと考えている。したがって胆管末端部に狭窄やくびれがみられるタイプと胆管末端部に狭窄やくびれがなく共通管へと移行するタイプの発生機序は異なるものと考えられる。共通管に関しては，これらの説からすると前者では膵管，後者では胆管ということになる。また共通管からしばしば膵管分枝が出ていることから共通管は膵管（Wirsung 管）あるいは胆管と腹側膵管の両者から形成されるとの意見もある[18,19]。これらの理由から合流形式に関して胆管膵管合流型（胆管合流型），膵管胆管合流型（膵管合流型）との表現を用いるべきでないとの意見もある[2]。

2．複雑型とは

古味[2]，戸谷ら[13]は複雑な合流形態を示し分類不能のものを複雑型とし，研究会の全国登録でも“その他の複雑な合流として”分類不能例を複雑型として登録するようになっている。複雑型に分類されるものには，膵管癒合不全や輪状膵などに合併した合流異常が含まれるが[20]，いずれも腹側膵と背側膵の癒合異常によるものである。新古味分類[11]ではこの複雑型に Warshaw ら[12]の膵管癒合不全の分類や副膵管の拡張を加えて細分しているが，複雑になりすぎ，輪状膵などすべてを網羅できないことから複雑型としてひとまとめにしておいた方がいいのではないかと思われる（図 4）。

3．共通管拡張型とは

現在，共通管拡張型の明確な定義はなく，各施設あるいは個人的な見解で判断が行われている。また共通管に蛋白栓がある時と消失した時では形態が変化することをしばしば経験する。すべてを明確に分類できるとはかぎらないが，われわれは“画像診断で合流部の胆管末端部に狭窄やくびれがみられ，合流部手前の胆

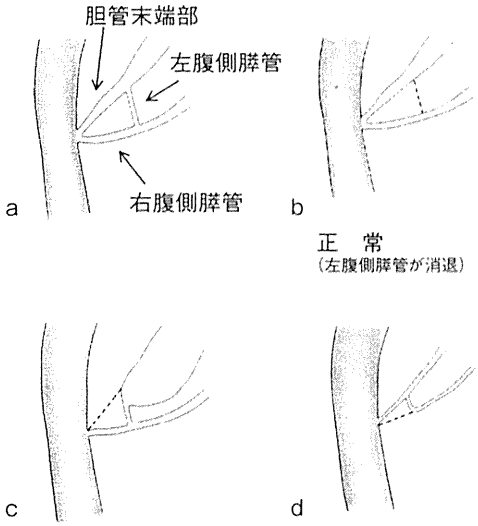

図 3　大井の説[16]に基づく膵・胆管合流異常の発生
a：総胆管を形成する肝憩室と左右腹側膵原基の２本の導管でつながっている。
b：左腹側膵原基が消退し正常の合流形態となる。
c：総胆管末端部が消退した結果，胆管が左腹側膵管と交通し胆管末端部に狭窄が形成され胆管拡張がある合流異常となる。
d：右腹側膵管が消退した場合には，胆管末端部に狭窄がなく胆管拡張が軽度の合流異常が発生する。

図 4　輪状膵に合併した合流異常
複雑な膵管形態を示し，十二指腸壁内憩室と膵管分枝の交通も認めた。

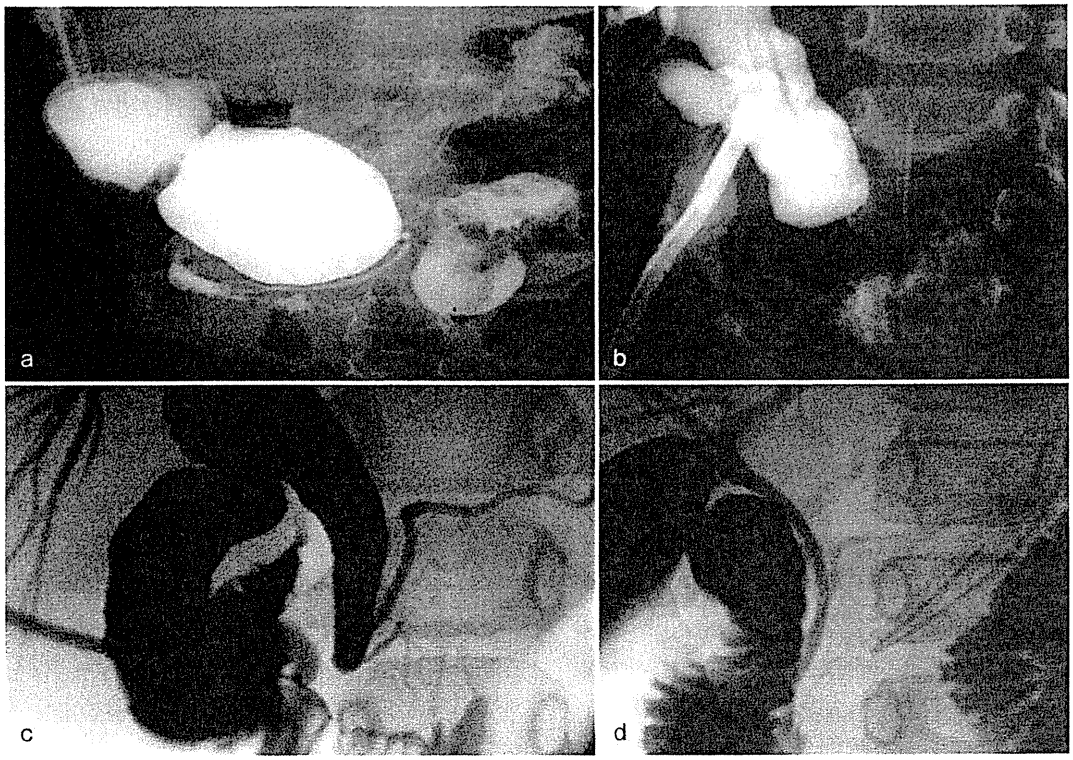

図 5　共通管非拡張例
a，b：拡張胆管末端の狭小部と膵管が合流する（胆管狭窄型）。
c：２本の膵管が合流している（胆管非狭窄型）。
d：胆管非拡張例（胆管非狭窄型）。

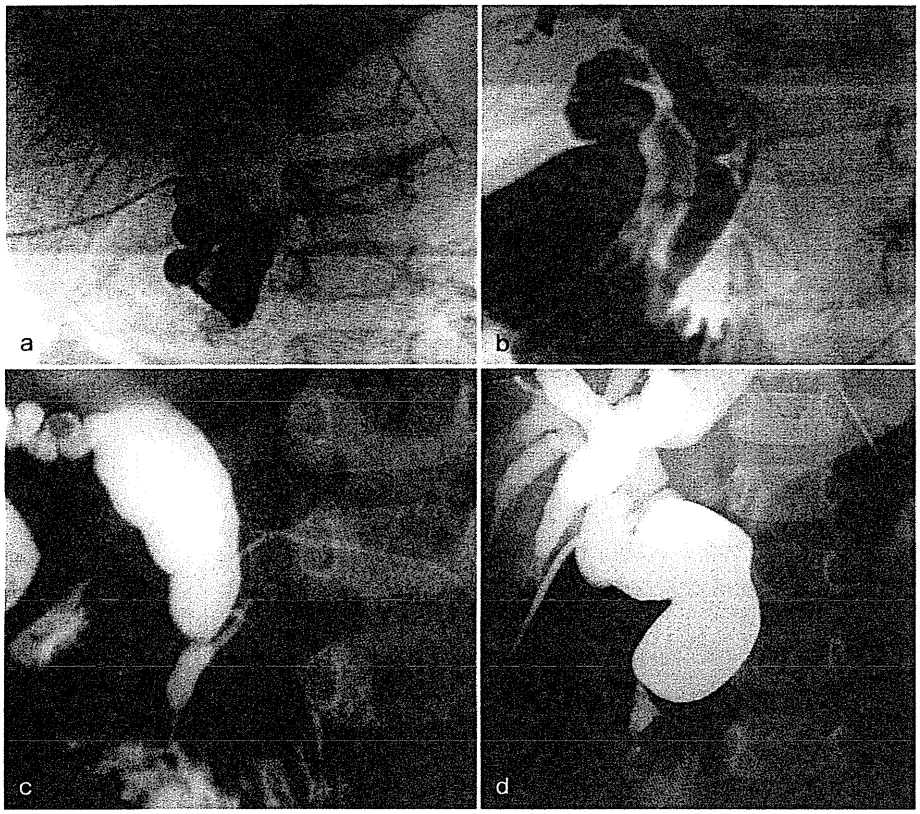

図 6　共通管拡張型．すべて胆管末端部に狭窄やくびれがある（胆管狭窄型）。
a，b：胆管の拡張は軽度だが，合流部手前にくびれがみられる。
c，d：胆管は嚢胞状拡張を示し，合流部手前に狭窄を認める。

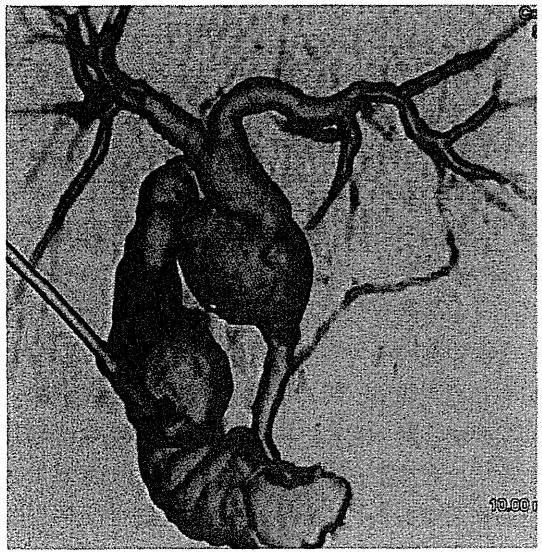

図 7　共通管拡張型あるいは非拡張型？
共通管に関しては尾側膵管に比べ拡張があるが，胆管拡張部から共通管にかけてスムーズに壁が移行し合流部直上の胆管との間に口径差を認めない（胆管非狭窄型）。われわれは共通管非拡張例に分類している。

管や膵管に比べ共通管に拡張がある症例”を共通管拡張型として定義している（図5，6）。たとえば図5cや図7を共通管拡張ありとするか非拡張とするかきっと判断がわかれると思われる。これらの症例はⅠc型の胆管拡張症で合流形式は膵管合流型（b型，胆管非狭窄型）である。共通管に関しては尾側膵管に比べると拡張があるが，胆管拡張部から共通管からにかけてスムーズに壁が移行し合流部直上の胆管との間に口径差を認めないことから非拡張型に分類している。今後，どのようなものを共通管拡張型とするか検討が必要である。

4．不全型（中間型）とは

古味[21]，戸谷ら[14]は中間型あるいは不全型の存在を提唱している。多くの先天性の形成異常に当てはまるように合流異常も不全型があって不思議でなく，膵管と胆管の合流には正常と異常との判別ができない症例も存在する。最近，成人では共通管が長く合流部に括約筋作用があるのに膵液の胆管内逆流がみられ，合流異常とよく似た病態を示す膵胆管高位合流症が報告[22]されている。小児での報告はなく先天性か後天性なのか乳頭機能不全などによるものか不明な点も多い。多発奇形をともなう症候群でしばしば不全型として分類されることがあるが，合流異常の型分類に追加する必要があるか今後の検討が必要である。

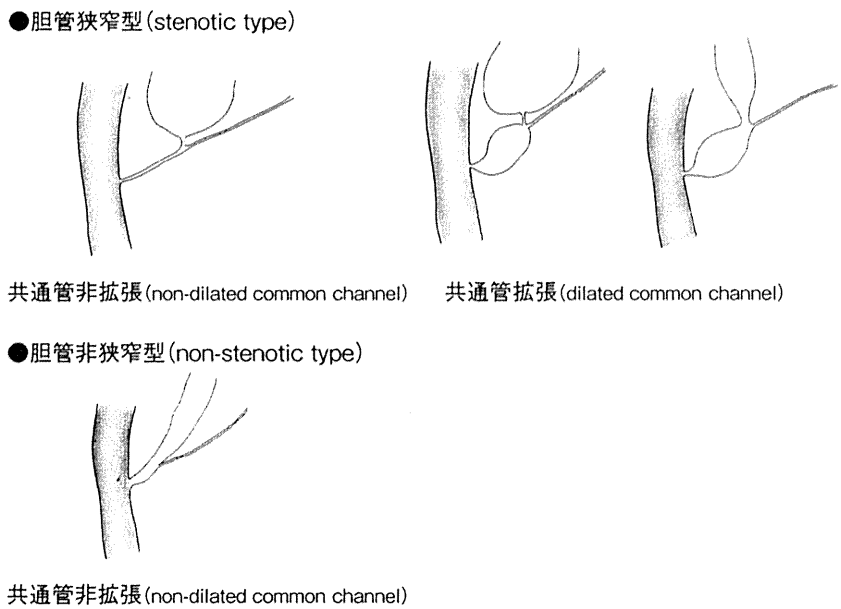

図 8 胆管末端部狭窄と共通管拡張に着目した膵・胆管合流異常の型分類

5．症状と合併症

土岐ら[23]による全国登録の解析では，急性膵炎や膵石を認める症例はａ型（胆管合流型）とｂ型（膵管合流型）は約20％で差がないが，ｃ型（複雑型）では約38％と高率に認めている。一方，共通管に注目すると共通管拡張例34％，共通管非拡張例17％で共通管拡張例に急性膵炎や膵石を約２倍高率に認めている。共通管拡張例で蛋白栓などによる閉塞性膵炎を合併しやすいことに異論はないと思われる。

6．治　療

手術では，ａ型（胆管合流型）ではほぼ全例に胆管末端部に狭窄部やくびれがみられること，また狭窄部より末梢側の狭小部が膵管とするなら膵内胆管は比較的容易に狭窄部あるいは合流部近くまで切除可能である。一方，胆管の拡張が軽度で胆管末端部に狭窄がないｂ型（膵管合流型）では膵内胆管を合流部手前まで切除することは困難で，また成人の胆管非拡張例では胆摘のみが行われることが多い。複雑型では膵管癒合不全，輪状膵など合併する膵疾患に対する治療が必要になることがある。この分類は手術の面から有用と思われるが，胆管の拡張形態や胆管末端部の狭窄と密接に関係している。

7．術後合併症

術後の膵炎，膵石は重要な問題であるが，これまでの報告をみると膵管癒合不全の合併，膵内遺残胆管，遺残結石，内瘻術後が多くの原因である。術後に共通管拡張例で膵炎や膵石形成が多いかは今後の検討課題である。自験例では術後膵炎の経験はなく頻度は少ないと考えている[24]。

8．著者の型分類に関する考え

合流異常の型分類は，膵管や胆管のどこに着目して分類を行うかで異なり，本症の多くで総胆管拡張症を伴うため総胆管の拡張形態や末端部の狭窄と密接に関係する。これまで提唱された合流異常の型分類は用語の違いだけのものもあり，誰にでもわかるような簡単な用語に統一する必要がある。簡単にまとめると着目点によって①膵管と胆管の合流形式に着目：胆管が膵管に合流し合流角度がほぼ直角の型，膵管が胆管に合流し合流角度が鋭角の型，複雑な型の３型，②胆管狭窄に着目：胆管末梢側に狭窄があり多くは総胆管が大きく拡張する型，胆管に狭窄がなく総胆管の拡張は軽度あるいは非拡張の型の２型，③共通管に着目：共通管拡張型と非拡張型の２型になるかと思われる。著者自身は，型分類において合流部手前の胆管狭窄やくびれの有無，共通管拡張の有無を取り入れた分類が発生学的にも臨床的にも有用と考えている。現在，われわれの施設では，“画像が直感的にイメージできること”から膵管と胆管の合流形式を直角型，鋭角型，複雑型の３型に分類し，それに共通管拡張，共通管非拡張を加えている。しかし胆管末端部の狭窄やくびれの有無が重要との観点から直角型は胆管狭窄型，鋭角型は胆管非狭窄型に変更したほうがいいように思われる。

表 1 胆管末端部の狭窄からみた臨床症状　自験 81 例

	胆管狭窄型 n＝48	胆管非狭窄型 n＝33	*P* value
腹痛*	28（58.3%）	30（90.1%）	＜.01
発熱	10（20.8%）	4（12.1%）	.31
腫瘤	2（4.2%）	0	.24
嘔吐*	18（37.5%）	22（66.7%）	＜.01
灰白便	3（0.06%）	0	
胎児診断	9（18.8%）	0	
高アミラーゼ血症*	23（47.9%）	27（81.8%）	＜.01
高ビリルビン血症	29（60.4%）	14（42.4%）	.11
肝酵素上昇	36（75%）	22（66.7%）	.41
蛋白栓，胆石	20（41.7%）	19（57.6%）	.16
胆道穿孔*	4（8.3%）	1（0.3%）	＜.05
膵浮腫，膵管拡張	5（10.4%）	5（15.2%）	.52
後膵炎	0	0	

＊有意差あり

表 2 共通管拡張からみた臨床症状　自験 81 例

	共通管拡張 n＝28	共通管非拡張 n＝53	*P* value
腹痛*	28（100%）	30（56.6%）	＜.001
発熱	4（13.4%）	10（18.9%）	.60
腫瘤	0	2（3.8%）	.30
嘔吐	18（64.8%）	22（41.5%）	.051
灰白便	1（3.6%）	2（3.8%）	.12
胎児診断	0	9（17.0%）	
高アミラーゼ血症*	23（89.3%）	27（50.9%）	＜.001
高ビリルビン血症	16（57.1%）	27（50.9%）	.59
肝酵素上昇	22（78.6%）	36（67.9%）	.31
蛋白栓，胆石*	20（71.4%）	19（35.8%）	＜.001
胆道穿孔*	4（14.3%）	1（1.9%）	＜.05
膵浮腫，膵管拡張*	8（28.6%）	2（3.8%）	＜.001
術後膵炎	0	0	

＊有意差あり

9．著者の分類案（図 8）

①胆管狭窄型（stenotic type）：合流部手前の総胆管末端部に狭窄やくびれがあり，胆管末端の狭小部と膵管がほぼ直角に合流しているようにみえる型。Ⅰaや Ⅳ-A 型の嚢胞状拡張例に多いが，紡錘または円筒状拡張のⅠc型にもみられる。従来の胆管合流型や直角型に相当すると思われる。

②胆管非狭窄型（non-stenotic type）：合流部手前の胆管末端部に狭窄やくびれがなく，胆管がスムーズに共通管に移行し胆管と膵管が鋭角に合流する型。胆管の拡張が軽度なⅠc型あるいは非拡張例にみられる。従来の膵管合流型や鋭角型に相当すると思われる。

③複雑型（complex type）：複雑な合流形態を示すもの。膵管癒合不全や輪状膵などが含まれる。

これに“合流部の胆管末端部に狭窄やくびれがあり，合流部手前の胆管や膵管に比べ共通管に拡張がある症例”の共通管拡張型（dilated common channel）と共通管非拡張型（non-dilated common channel）を追加する。

これは旧古味分類[4]と戸谷らの分類[13]を参考に“合流部手前の胆管狭窄”と“共通管拡張”に着目した分類である。この分類では，共通管拡張例のほとんどが胆管狭窄型や複雑型に認めることになり，新古味分類の Type Ⅱb の胆管非狭窄型（鋭角型）は共通管非拡張型になるところに違いがある。

この分類に基づいて，われわれの施設で過去 15 年間に経験した 15 歳以下の合流部の評価可能で複雑型を除いた 81 例を対象とした胆管末端部の狭窄の有無と共通管の拡張の有無での臨床的特徴を簡単に示す。胆管狭窄型に比べ胆管非狭窄型に有意に腹痛，高アミラーゼ血症が多くみられたが，蛋白栓，胆石の合併には有意差を認めなかった（表 1）。一方，共通管に注目すると共通管拡張例では有意に腹痛，高アミラーゼ血症，蛋白栓・胆石の合併が多くみられた（表 2）。

おわりに

小児では侵襲的なERCPが省かれる傾向にあり，直接膵管造影を必要とする複雑な分類には無理がある。さまざまな意見があると思われるが，これまでの研究会での登録事業も活用できる型分類がいいのではないかと思われる。また明確な型分類ができない症例もあると思われるが，共通管拡張型とはどのような症例かなど研究者間で用語の共通の定義が必要で同じ定義を持って症例を型分類し検討する必要がある。

参考文献

1) Todani T, Narusue M, Watanabe Y, et al.: Congenital bile duct cyst: its classification, operative procedures, and review of 37 cases including cancer arising from Choledochal cyst. Am J Surg **134**: 263-269, 1977.
2) 古味信彦：合流形式と分類．膵・胆管合流異常そのConsensusとControversy．古味信彦監，船曳孝彦編，64-73，医学図書出版，1997.
3) 石原　慎，堀口明彦，宮川修一：合流形式と分類．膵・胆管合流異常の新たな展開．高田忠敬監，青木達哉，土田明彦編，7-11，医学図書出版，2011.
4) Komi N, Udaka H, Ikeda N, et al.: Congenital dilatation of the biliary tract: New classification and study with particular reference to anomalous arrangement of the the pancreaticobiliary ducts. Gastroenterol Jpn **12**: 293-304, 1977.
5) 木村邦夫：成人における先天性総胆管拡張症28症例の検討（胆管像および胆管・膵管合流様式と病態について）．日消病会誌 **73**: 401-414，1976.
6) Kimura K, Ohto M, Ono T, et al.: Congenital cystic dilatation of the common bile duct: relationship to anomalous pancreaticobiliary ductal union. Am J Roentgenol **128**: 571-577, 1977.
7) 大井　至，原　俊明：EPCGからみた膵・胆管合流異常．小児外科 **9**: 1121-1129，1977.
8) 土岐文武，大井　至，今泉俊秀，ほか：ERCPによる膵胆道形態の特徴．消化器画像 **5**: 205-214，2003.
9) 藤井秀樹，板倉　淳，平井　優，ほか：先天性胆道拡張症と膵・胆管合流異常の発生とその概念．胆と膵 **29**: 881-888，2008.
10) 川内康裕，岡部郁夫，越永従道：先天性胆道拡張症における膵管形態の検討．小児外科 **24**: 105-114，1992.
11) Komi N, Takehara H, Kunitomo K, et al.: Does the type of anomalous arrangement of pancreaticobiliary ducts influence the surgery and prognosis of Choledochal cyst? J Pediatr Surg **27**: 728-731, 1992.
12) Warshaw AL, Simeone JF, Schapiro RH, et al.: Evaluation and treatment of the dominant dorsal duct syndrome (Pancreas divisum redefined). Am J Surg **159**: 59-64, 1990.
13) Todani T: Congenital choledochal dilatation: Classification, clinical features, and long-term results. J Hep Bil Pancr Surg **4**: 276-282, 1997.
14) 戸谷拓二，渡辺泰宏：胆道拡張症の分類と合流異常の分類．第36回日本膵・胆管合流異常研究会プロシーディングス **36**: 44-45，2013.
15) Odgers PNB: Some observations on the development of the ventral pancreas in man. J Anat **65**: 1-7, 1930.
16) 大井　至：腹側膵の発生と膵・胆管合流異常．胆と膵 **17**: 723-729，1996.
17) Suda K, Matsumoto Y, Miyano T: Narrow duct segment distal to Choledochal cyst. Am J Gastroenterol **86**: 1259-1263, 1991.
18) 松本由郎，藤井秀樹，板倉　淳，ほか：膵・胆管合流異常の発生とその基盤—腹側膵の発生と膵・胆管合流異常—．胆と膵 **17**: 731-739，1996.
19) 神澤輝実，来間佐和子，原　精一，ほか：膵・胆管合流異常の概念・発生を巡る問題点．胆と膵 **34**: 209-215，2013.
20) Urushihara N, Fukumoto K, Fukuzawa H, et al.: Recurrent pancreatitis caused by pancreatobiliary anomalies in children with annular pancreas. J Pediatr Surg **45**: 741-746, 2010.
21) 古味信彦：膵管胆道合流異常の中間型（亜型）の提唱．外科治療 **54**: 108-109，1986.
22) Kamisawa T, Suyama M, Fujita N, et al.: Pancreatobiliary reflux and the length of a common channel. J Hepatobiliary Pancreat Sci **17**: 865-870, 2010.
23) 土岐　彰，鈴木淳一，渡井　有，ほか：先天性胆道拡張症，膵・胆管合流異常の各種分類法は本当に役立っているのか？　胆と膵 **33**: 17-22，2012.
24) Urushihara N, Fukumoto K, Fukuzawa H, et al.: Long-term outcomes after excision of choledochal cysts in a single institution: operative procedures and late complications. J Pediatr Surg **47**: 2169-2174, 2012.

*　　*　　*

Clinica Chimica Acta 440 (2015) 49–54

Contents lists available at ScienceDirect

Clinica Chimica Acta

journal homepage: www.elsevier.com/locate/clinchim

Negative feedback loop of cholesterol regulation is impaired in the livers of patients with Alagille syndrome

Yuki Miyahara [a], Kazuhiko Bessho [a], Hiroki Kondou [a,*], Yasuhiro Hasegawa [a], Kie Yasuda [a], Shinobu Ida [b], Yoshiyuki Ihara [c], Koichi Mizuta [c], Yoko Miyoshi [a], Keiichi Ozono [a]

[a] Department of Pediatrics, Osaka University Graduate School of Medicine, 2–2 Yamada-oka, Suita City, Osaka, Japan
[b] Department of Pediatric Gastroenterology, Nutrition and Endocrinology, Osaka Medical Center and Research Institute for Maternal and Child Health, 840 Murodou, Izumi City, Osaka, Japan
[c] Department of Transplant Surgery, Jichi Medical University, 3311–1 Yakushiji, Shimotsuke City, Tochigi, Japan

ARTICLE INFO

Article history:
Received 22 March 2014
Received in revised form 6 October 2014
Accepted 24 October 2014
Available online 31 October 2014

Keywords:
Alagille syndrome
Hypercholesterolemia
Low-density lipoprotein receptor
Scavenger receptor class B type I
3-hydroxy-3-methylglutaryl coenzyme A reductase

ABSTRACT

Aim: To characterize cholesterol regulation in the liver of patients with Alagille syndrome (AGS).
Methods: Serum total cholesterol (TC) and total bile acid (TBA) levels were measured in 23 AGS patients. The expressions of genes involved in cholesterol regulation, including low-density lipoprotein receptor (*LDLR*), scavenger receptor class B type I (*SR-BI*), 3-hydroxy-3-methylglutaryl coenzyme A reductase (*HMGCR*), cholesterol 7α-hydroxylase (*CYP7A1*), ATP-binding cassette transporter (*ABC*) *A1*, and *ABCG1/5/8*, were measured in liver tissues from five of these patients. Expression of regulators for these genes, including farnesoid X receptor/small heterodimer partner (*SHP*), liver X receptor α (*LXRα*) and mature Sterol regulatory element-binding protein 2 (SREBP2) was measured. The expression of mature SREBP2 protein was also examined.
Results: Serum TC and TBA levels were correlated in the AGS patients. Liver cholesterol was also increased compared with controls, and correlated with bile acid contents. *LDLR*, *SR-BI*, *HMGCR*, and *ABCGs* mRNA expression were upregulated, while *CYP7A1* mRNA expression was downregulated in AGS livers. *SHP* and *LXRα* mRNA expression was also increased, but maturation of SREBP2 was not suppressed in the patients.
Conclusions: The major upregulators of liver cholesterol might be increased in AGS patients, indicating an impaired negative feedback mechanism and accelerated liver cholesterol accumulation.

1. Introduction

Cholestatic disorders often accompany profound hypercholesterolemia [1–4]. Such distinct lipid abnormalities may unfavorably affect development and nutrition in childhood. Hypercholesterolemia generally predisposes patients to cardiovascular diseases, particularly atherosclerosis. It has been hypothesized that advanced liver damage leads to a considerable decrease in high-density lipoprotein (HDL), which is protective against atherogenesis. Decreased HDL in the face of hypercholesterolemia will likely engender atherosclerosis. Therefore, the adverse effects of increased plasma cholesterol have been extensively studied in patients with cholestatic disorders [5–7]. However, uniform results have not been obtained.

Alagille syndrome (AGS) is a rare hereditary cholestatic disorder primarily caused by mutations in *JAGGED1* (*JAG1*), a ligand of the Notch signaling pathway [8–13]. The cholestasis is thought to result from intrahepatic bile duct paucity. This disorder also presents various extrahepatic manifestations such as peripheral pulmonary stenosis, butterfly-like vertebrae, peculiar face, and ocular posterior embryotoxon [11–13]. In addition, children with AGS presenting cholestasis usually exhibit profound hypercholesterolemia and present with failure to thrive [14, 15]. However, limited information is available on the liver cholesterol regulatory system in this disease [3].

This study aimed to characterize cholesterol regulation in the liver of AGS patients by examining mRNA expression of major liver cholesterol regulatory proteins such as low-density lipoprotein receptor (*LDLR*), 3-hydroxy-3-methylglutaryl coenzyme A reductase (*HMGCR*), and scavenger receptor class B type I (*SR-BI*). Concurrent expression of liver nuclear receptors such as farnesoid X receptor (*FXR*, *NR1H4*) and liver X receptor α (*LXRα*, *NR1H3*), which control liver cholesterol regulatory proteins, was also examined (Fig. 1) [16–19]. Furthermore, as a translational regulator of *HMGCR* and *LDLR*, mature sterol regulatory element-binding protein 2 (SREBP2) was examined [20–22]. Our results demonstrate a one-way positive feedback of cholesterol regulation in

Abbreviations: AGS, Alagille syndrome; BA, biliary atresia; TC, total cholesterol; TBA, total bile acids; LDLR, low-density lipoprotein receptor; HDL, high-density lipoprotein; SR-BI, scavenger receptor class B type I; HMGCR, 3-hydroxy-3-methylglutaryl coenzyme A reductase; FXR, farnesoid X receptor; LXRα, liver X receptor α; CYP7A1, cholesterol 7α-hydroxylase; SHP, small heterodimer partner; SREBP2, sterol regulatory element-binding protein 2.

* Corresponding author. Tel.: +81 6 6879 3932.
E-mail address: kondou@ped.med.osaka-u.ac.jp (H. Kondou).

http://dx.doi.org/10.1016/j.cca.2014.10.034
0009-8981/

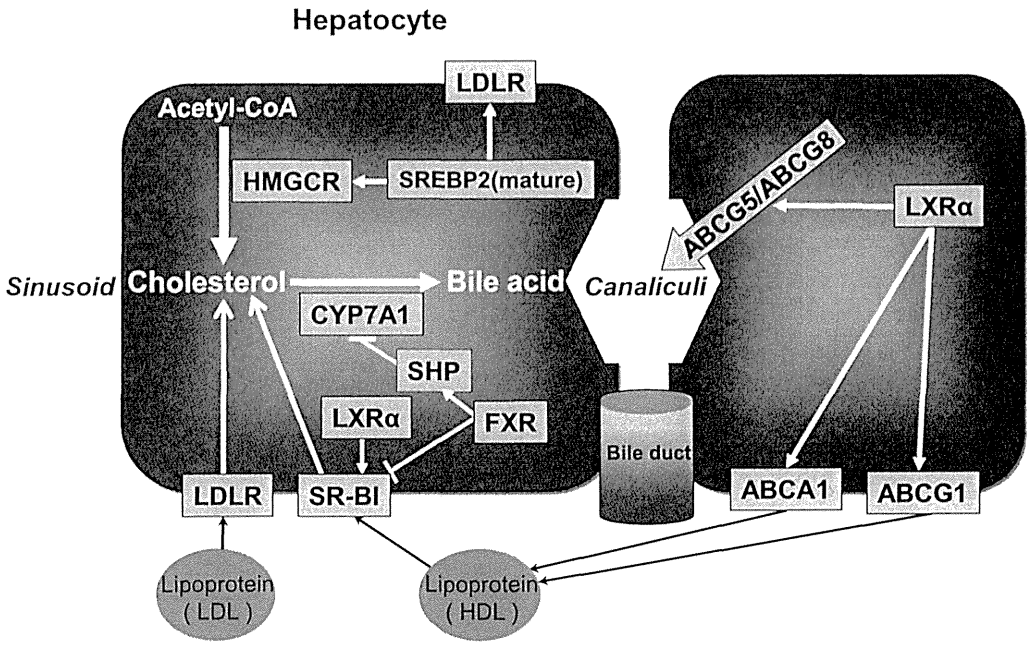

Fig. 1. The cholesterol regulatory system in hepatocyte. LDLR, low-density lipoprotein receptor; SR-BI, scavenger receptor class B type I; HMGCR, 3-hydroxy-3-methylglutaryl coenzyme A reductase; CYP7A1, cholesterol 7a-hydroxylase; FXR, farnesoid X receptor; SHP, small heterodimer partner; LXRα, Liver X receptor α; ABCA1, ATP-binding cassette transporters A1; ABCG1, ATP-binding cassette transporters G1; ABCG5/8, ATP-binding cassette transporters G5/8, SREBP2(mature); cleaved form of sterol regulatory element-binding protein 2.

cholestatic AGS livers, which results in higher liver cholesterol content and leads to profound hypercholesterolemia.

2. Patients and methods

2.1. Patients enrolled in the preliminary study to evaluate the impact of cholestasis on plasma cholesterol

Twenty-three AGS patients who had been followed at Osaka University Hospital, Osaka Medical Center and Research Institute for Maternal and Child Health, and Jichi Medical University (female/male, 10/13; age, 5 months–20 years) were enrolled in the preliminary study to explore the correlation between their serum total bile acid (TBA) and serum total cholesterol (TC) levels and evaluate the influence of cholestasis on serum cholesterol. Biochemical data were retrospectively collected from the patients' medical records.

AGS was diagnosed by the presence of cholestasis with specific liver histology demonstrating a paucity of interlobular bile ducts and the fulfillment of at least 3 of the following diagnostic criteria: cholestasis, heart disease, peculiar face, butterfly-like vertebrae, and posterior embryotoxon [11,12]. Genotyping of *JAG1* gene was performed to further confirm the diagnosis by direct sequencing of all exons.

2.2. AGS patients enrolled in the study of liver cholesterol regulation

Among the 23 AGS patients, five underwent living related liver transplantation because of liver failure and severe pruritus. Liver tissues were harvested from these patients at the time of liver transplantation, snap frozen in liquid nitrogen, and stored at −80 °C until analysis.

Six control liver tissues without cholestasis and dyslipidemia were also obtained from two patients with hemangioma, three patients with hepatoblastoma and a patient with ornithine transcarbamylase deficiency. Non-tumorous tissues away from the tumors were isolated from the liver obtained at the time of liver transplantation or lobectomy, and all of the isolated tissue showed normal histology. The background and biochemical data of each control patient were shown in Supplementary Tables 1 and 2. This study was approved by the relevant institutional medical ethics review boards. Informed consent was obtained from the parents of the enrolled children before study initiation.

2.3. Correlation between serum TC and TBA in AGS patients

To evaluate the influence of cholestasis on serum cholesterol levels, we examined the correlation between serum TC and serum TBA levels in the 23 AGS children.

Lipid and bile acids were extracted from the liver tissue according to the method described by Folch et al. [23] and Beher WT et al. [24]. TC and TBA levels were measured using the LabAssay cholesterol assay kit (Cayman Chemical, Ann Arbor, MI, USA) and the total bile acids assay kit (Diazyme Laboratories, Poway, CA, USA), respectively, according to the manufacturer's protocol.

2.4. Quantitative real-time polymerase chain reaction (qRT-PCR)

We examined the mRNA expression of proteins/enzymes and liver nuclear receptors involved in the liver cholesterol regulatory system (Fig. 1) [16–19]. Total hepatic RNA was isolated from frozen liver tissue using the RNeasy Mini Kit (Qiagen, Hilden, Germany) according to the manufacturer's protocol.

One microgram of total RNA was reverse transcribed using the ReverTra Ace® qRT-PCR Kit (TOYOBO LIFE SCIENCE, Osaka, Japan). For the quantification of *CYP7A1* mRNA, we used Taqman® real-time quantitive PCR (Applied Biosystems, Foster City, CA, USA), and for other genes, we used SYBR® Green real-time quantitative PCR (Applied Biosystems, Foster City, CA, USA). All PCR procedures were performed using the ABI 7900 Fast Real-Time PCR system (Applied Biosystems, Foster City, CA, USA). The relative mRNA levels were normalized to *GAPDH* expression, and the fold changes were determined using the $2^{-\Delta\Delta Ct}$ method. We performed melting curve analysis and confirmed that single amplicon with an expected melting temperature was generated in each reaction (supplementary figure). The primer sets used in qRT-PCR are listed in Table 3.

We evaluated the mRNA expression of lipoprotein receptors, including *LDLR* and scavenger receptor class B type I (*SR-BI*), which promote

Table 1
Backgrounds of the 5 patients, their liver histologies, and Child–Pugh classifications at liver transplantation.

Patients	Age at OLT	Gender	Phenotypic anomalies				Xanthoma	POD	Mutations *in JAGGED1* gene	Treatment	Indication for LT	Child–Pugh classification
			Cardiac	Face	Vertebrae	Eye						
1	1y2m	F	+	+	+	−	+	+	Not Detected	LT	FTT	C
2	1y10m	M	+	+	+	+	+	+	c177_178insG p.A60G fsx13	LT	FTT	B
3	1y2m	F	+	+	+	−	+	+	c.1486delT p.C496VfsX2	Kasai, LT	FTT	C
4	1y5m	M	+	+	−	−	+	+	c.G233A p.C78Y	Kasai, LT	FTT	B
5	2y7m	M	+	+	+	−	+	+	c.695_755del p.A232Gfsx160	Kasai, LT	Pruritus	B

LT, liver transplantation; FTT, failure to thrive; POD, paucity of interlobular bile duct.

liver LDL and HDL uptake. The mRNA expression of *HMGCR* as a limiting enzyme in the cholesterol biosynthetic pathway was also examined. Simultaneously, we determined the expression of sterol regulatory element-binding protein 2 (*SREBP2*), which plays a central role in the enhancement of *HMGCR* and *LDLR* expression [21,22,25]. The expression of SREBP cleavage-activating protein (*SCAP*) and insulin-induced genes 1 and 2 (*INSIG-1* and *2*), which regulate the maturity of SREBP2 [21,22] was also examined. The expression of cholesterol 7α-hydroxylase (*CYP7A1*), a rate-limiting enzyme in bile acid synthesis from cholesterol was examined. Among the cholesterol transporters, the expression of ATP-binding cassette transporter (*ABC*) *A1* and *ABCG1*, which excrete cholesterol from hepatocytes into the circulation, and *ABCG5* and *ABCG8*, which excrete cholesterol from hepatocytes into the bile canaliculi, was examined (Fig. 1) [16–18].

Among the liver nuclear receptors, mRNA expression of *FXR* and small heterodimer partner (*SHP*, *NR0B2*), which are known to down-regulate *CYP7A1* and *SR-BI* expression, and *LXRα*, which is an oxysterol receptor and upregulates *ABCA1* and *ABCG1/5/8*, was evaluated (Fig. 1) [16–19,26,27].

2.5. Western blotting

Frozen liver tissues were homogenized in lysis buffer containing a mixture of 500 mM Tris–HCl (pH, 7.4), 1% Nonidet P-40, 0.25% deoxycholic acid-Na, 150 mM NaCl, 1 mM ethylene diamine tetra acetate, and a protease inhibitor cocktail (Roche Diagnostics, Mannheim, Germany). Homogenates were centrifuged at 12,000 *g* for 20 min, and the supernatants were collected as protein samples. Protein levels were determined using the DC protein assay kit (Bio-Rad Laboratories, Hercules, CA, USA). Equal amounts of protein were separated by 10% sodium dodecylsulfate polyacrylamide gel electrophoresis (SDS-PAGE) and transferred to nitrocellulose membranes. Membranes were blocked in 5% bovine serum albmin in Tris-buffered saline (TBS). The membranes were then immunoblotted with anti-SREBP2 (1:800; Abcam, Cambridge, MA, USA) or anti-β-actin (1:4,000; Sigma Chemical, St Louis, MO, USA) and developed with horseradish peroxide-conjugated secondary antibody (Promega, Madison, WI, USA), followed by enhancement with SuperSignal West Dura extended duration substrate antibodies (Pierce, Rockford, IL, USA). The protein bands were digitally imaged for densitometry using ImageJ (National Institutes of Health, Bethesda, MD, USA).

2.6. Statistical analysis

All results are presented as mean ± SEM. The correlation between serum TC and TBA levels was estimated using Pearson's test. Differences between groups were calculated using two-tailed Student's *t*-test using Prism software (GraphPad Software, Inc., La Jolla, CA). A *p*-value of <0.05 was considered statistically significant.

3. Results

3.1. Relationship between serum TBA and TC levels

Serum TC levels showed a significant correlation with serum TBA levels in AGS patients ($p < 0.001$; Fig. 2).

3.2. Liver cholesterol and bile acid contents

The liver is the primary organ contributing to cholesterol homeostasis; therefore, to explore the potential mechanisms underlying the constant TC to TBA ratio in serum of AGS patients, we measured cholesterol and bile acid contents in the liver tissue from the 5 AGS patients who underwent liver transplantation. As shown in Tables 1 and 2, all of the 5 patients fulfilled the diagnostic criteria of AGS (11–13), and showed prominent hypercholesterolemia along with cholestasis and jaundice. Cholesterol and bile acid levels in the livers from the AGS patients were significantly increased by approximately two-fold compared with those in the normal control ($p < 0.05$ for both; Table 4). The liver cholesterol content significantly correlated with the bile acid content in the AGS group ($p < 0.05$).

3.3. mRNA expression of cholesterol regulatory proteins in the liver

Because cholesterol accumulates in the livers of AGS patients with hypercholesterolemia, we examined hepatic mRNA expression of cholesterol regulatory proteins in AGS livers.

mRNA expressions of *HMGCR*, *LDLR*, and *SR-BI* were significantly increased by 2.3-, 2.5-, and 4.9-fold, respectively, in the AGS group compared to the control group ($p < 0.05$; Fig. 3a).

With regard to bile acid metabolism, mRNA expression of *CYP7A1*, a rate-limiting key enzyme for bile acid synthesis, was decreased significantly in the AGS group ($p < 0.05$).

Table 2
Serum liver function tests at liver transplantation.

Patient	T-Cho (mg/dl)	LDL-C (mg/dl)	HDL-C (mg/dl)	TB (mg/dl)	DB (mg/dl)	TBA (μmol/l)	AST (U/l)	ALT (U/l)	Albumin (g/dl)	PT INR
1	1600	1267	19	9.0	7.3	589	153	173	2.5	1.36
2	1354	ND	ND	17.6	12.91	734	215	148	4.1	1.01
3	1245	1168	47	8.4	6.9	624	348	212	1.9	1.65
4	692	540	20	12.1	9.9	241	247	91	2.9	1.2
5	688	ND	ND	10.2	6.53	301	157	145	3.8	0.98
normal	107–190	55–110	34–80	0.3–1.4	0.0–0.5	2–10	<40	<40	3.8–4.9	0.80–1.20

T-Cho, total cholesterol; LDL-C, low-density lipoprotein cholesterol; HDL-C, high-density lipoprotein cholesterol; TB, total bilirubin; DB, direct bilirubin; TBA, total bile acids; AST, aspartate aminotransferase; ALT, alanine aminotransferase; PT-INR, international normalized ratio of prothrombin time; ND, not determine. LDL-C and HDL-C were measured using the Cholestest® LDL and the Cholestest®N HDL (SEKISUI MEDICAL, Tokyo, JAPAN), respectively.

Table 3
Primer sets for RT-PCR.

Genes	Forward (5′-3′)	Reverse (5′-3′)
HMGCR	ATA GGA GGC TAC AAC GCC CAT	TTC TGT GCT GCA TCC TGT CC
SREBP2	CAG CTG CAC ATC ACA GGG AA	GTA CAT CGG AAC AGG CGG AT
SCAP	GGG AAC TTC TGG CAG AAT GAC T	CTG GTG GAT GGT CCC AAT G
INSIG1	ATC TTT TCC TCC GCC TGG T	GGG GTA CAG TAG GCC AAC AA
INSIG2	TTC CTC TAT GTT CGT TCT TGG TT	TTT CTG CGA TAA CTT TAC ATT CGT
LDLR	CAA TGT CTC ACC AAG CTC T	TCT GTC TCG AGG GGT AGC T
SRB1	TCT ACC CAC CCA ACG AAG GCT	CCT GAA TGG CCT CCT TAT CCT
LXRα	AAG CCC TGC ATG CCT ACG T	TGC AGA CGC AGT GCA AAC A
FXR	CTC ATT GAA CAT TCC CAT TTA CCT ACC	GGA CCT GCC ACT TGT TCT GTT A
SHP	CCA TCC TCT TCA ACC CCG A	CGG AAT GGA CTT GAG GGT G
ABCA1	TCG ACA TGG TGA AAA ACC AG	AAT GGT GAC ACA AAG CGA TTC
ABCG1	TCA GGG ACC TTT CCT ATT CG	TTC CTT TCA GGA GGG TCT TGT
ABCG5	TCT CTT GGC CCC CCA CTT A	CTA TAT TTG GAT TTT GGA CGA TAC CA
ABCG8	GAC AGC TTC ACA GCC CAC AA	GCC TGA AGA TGT CAG AGC GA
GAPDH	GAA GGT GAA GGT CGG AGT C	GAA GAT GGT GAT GGG ATT TC

HMGCR, 3-hydroxy-3-methylglutaryl coenzyme A; *SREBP2*, sterol regulatory element-binding protein 2.
SCAP, SREBP cleavage-activating protein; *INSIG1*, insulin-induced genes 1; *INSIG2*, insulin-induced genes 2.
LDLR, low-density lipoprotein receptor; *SR-BI*, scavenger receptor class B type I; *LXRα* Liver X receptor α.
FXR, farnesoid X receptor; *SHP*, small heterodimer partner; *ABCA1*, ATP-binding cassette transporters A1.
ABCG1, ATP-binding cassette transporters G1; *ABCG5*, ATP-binding cassette transporters G5.
ABCG8, ATP-binding cassette transporters G8; *GAPDH*, glyceraldehyde-3-phosphate dehydrogenase.

Among the cholesterol transporters, mRNA expression of *ABCG5* and *ABCG8* was increased in the AGS group by 6.7- ($p < 0.01$) and 3.4-fold ($p < 0.01$), compared to the control group, respectively. mRNA expression of *ABCG1* was also significantly increased, while *ABCA1* mRNA remained unchanged.

3.4. mRNA expression of liver nuclear receptors controlling cholesterol regulatory proteins

In the AGS group, *SHP* mRNA expression, but not *FXR* mRNA expression, was significantly increased ($p < 0.05$; Fig. 3b). AGS livers also showed high *LXRα* mRNA expression, which was 5.7-fold compared to that in the control livers ($p < 0.01$).

3.5. Expression of intracellular cholesterol regulatory proteins

The above data suggested dysregulation of the negative feedback loop in cholesterol homeostasis in AGS livers. Therefore, we examined

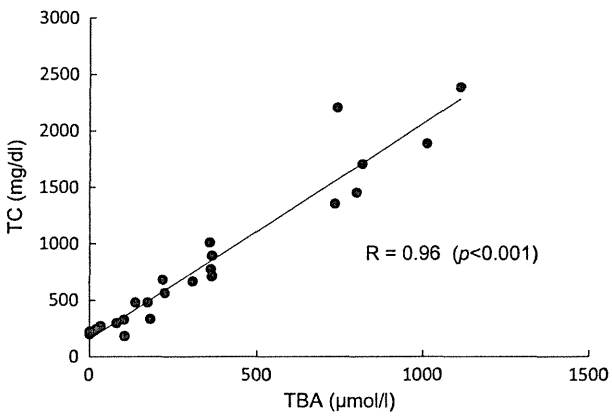

Fig. 2. Scatter plot of serum total cholesterol (TC) against serum total bile acid (TBA) levels.

Table 4
Hepatic cholesterol and bile acids concentrations in the livers.

	Control liver	AGS liver
Total cholesterol (mg/g liver)	1.27 ± 0.46	2.91 ± 0.49*
Total bile acids (μmol/g liver)	0.10 ± 0.05	0.39 ± 0.05†

Means ± SEMs are given.
The liver cholesterol content was significantly correlated with the bile acid content in AGS group ($p < 0.05$).
* $p < .05$, significantly different from control livers.
† $p < .01$, significantly different from control livers.

the expression of the key elements of intracellular cholesterol regulation [20]. Despite cholesterol accumulation in the liver, mRNA expression of *SREBP2*, *SCAP*, and *INSIG-2* was not decreased, while that of *INSIG-1* was significantly increased (Fig. 4a). The expression of mature SREBP2 protein was not suppressed in AGS livers (Fig. 4b).

4. Discussion

In this study, we performed comprehensive analyses to clarify the liver cholesterol regulatory system in AGS children with profound hypercholesterolemia. Many previous studies have demonstrated that liver nuclear receptors such as FXR, SHP, and LXR are activated by bile acids or oxysterols and change the respective downstream bile acid or cholesterol regulatory pathways [16–19,25–28]. However, analyses of the cholesterol regulatory system in human livers with cholestasis are scarce [3,29]. The plasma lipoprotein profiles in AGS have been documented in many earlier reports [1,3,4,6], but information on cholesterol regulators in the liver that control hepatic and serum cholesterol levels is limited. Therefore, the results of this study may lead to a better understanding of liver cholesterol regulation under cholestasis.

This study confirmed that serum TC and TBA levels were strongly correlated and that liver cholesterol and bile acid contents were considerably increased, with a significant correlation, in AGS children.

Enjoji et al. documented that mRNA expression of *LDLR* was decreased in livers with primary biliary cirrhosis, which was also characterized by cholestasis and hypercholesterolemia [29]. Furthermore, Nagasaka et al. documented that SR-BI protein expression is decreased in AGS livers with rather mild cholestasis [3]. These studies used liver tissues from patients in early stages that showed mild liver damage. In this context, we speculated that the expression of the major upregulators of liver cholesterol may decrease because of a negative feedback loop. However, the study provided contradicting results; increased liver expression of *HMGCR*, *LDLR*, and *SR-BI* may further enhance hepatic cholesterol accumulation in AGS children. Several experiments using animal models have shown that severe cholestasis induces high *HMGCR* expression in the liver, thus contributing to hypercholesterolemia [4,30]. The expression and activity of liver cholesterol regulators may differ with the severity of cholestasis.

HMGCR and *LDLR* expression are regulated by the SREBP2 transcription factor [21,22,25]. *SREBP2* mRNA is transcriptionally suppressed by LXRα, and the protein is processed into a mature form by SCAP and INSIG-1and 2 in response to a decrease in cellular cholesterol levels [16–18,25]. In this study, *LXRα* mRNA was considerably increased in AGS livers (Fig. 3b). However, *SREBP2* mRNA expression was not suppressed (Fig. 4a). Furthermore, the expression of mature SREBP2 was also not suppressed in AGS livers despite increased liver cholesterol content and *INSIG-1* mRNA expression (Fig. 4b). These results indicated that negative feedback for liver cholesterol content was abrogated in AGS children. An explanation for this dysregulation in SREBP2 expression and maturation remains elusive.

In contrast to elevated *HMGCR*, *LDLR*, and *SR-BI* expression, the liver expression of *CYP7A1* as a limiting enzyme of bile acid synthesis was decreased in AGS children. Therefore, it is likely that a decrease in the conversion from cholesterol to bile acid also contributes, at least to some extent, to the high cholesterol content in the liver of AGS children.

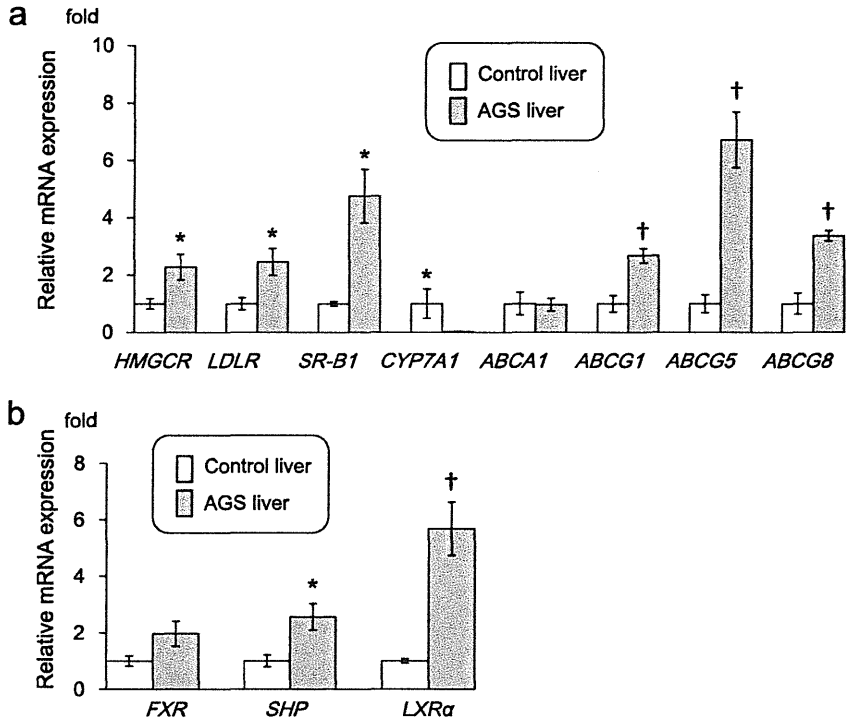

Fig. 3. Liver mRNA expression of cholesterol regulators and nuclear receptors in five patients with Alagille syndrome (AGS; gray bar) and five controls without cholestasis and hyperlipidemia (white bar). The expression of each gene is represented as a fold-change as compared to that in the control livers after normalization to *GAPDH*. n = 6 samples for control group; n = 5 samples for AGS group. $^{*}p < 0.05$; $^{\dagger}p < 0.01$ between groups.

Among the nuclear receptors controlling liver cholesterol regulators, *LXRα* and *SHP* mRNA expression was increased (Fig. 4b). We could infer that the enhancement of the FXR-SHP pathway led to the suppression of *CYP7A1* expression and that an increase in *LXRα* expression led to the upregulation of *SR-B1* and *ABCGs 1, 5,* and *8* (Fig. 1) [16–19,26–28]. However, *ABCA1* expression, which should also be upregulated by LXRα, remained unchanged [16–18]. Therefore, changes in liver cholesterol regulators were not exclusively regulated by changes in the expression of known liver nuclear factors.

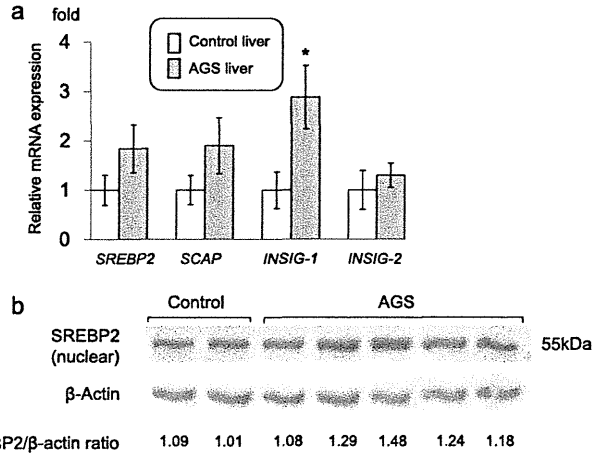

Fig. 4. Expression and maturation of the key elements of intracellular cholesterol regulation. A: mRNA expression of sterol regulatory element-binding protein 2 (*SREBP2*), SREBP cleavage-activating protein (*SCAP*), and insulin-induced genes 1 and 2 (*INSIG-1* and *2*). The expression of each gene is represented as a fold-change as compared to that in the control livers after normalization to *GAPDH*. n = 6 samples for control group; n = 5 samples for AGS group. $^{*}p < 0.05$ between groups. B: Protein expression of mature SREBP2. The signal intensity of the SREBP2 protein in the truncated form (55 kDa) relative to that of β-actin is shown in the panel. AGS, Alagille syndrome.

Taken together, this study demonstrated that the negative feedback regulation of liver cholesterol levels was impaired in children with AGS. Despite the upregulation of hepatic LDLR and SR-BI, both of which remove lipoproteins from the circulation, AGS children exhibit profound hypercholesterolemia. Increased expression of *HMGCR* may greatly contribute to the profound hypercholesterolemia. Alternatively, under intrahepatic bile duct paucity, increased amounts of cholesterol in bile canaliculi possibly resulting from increased ABCG5/8 expression, may enter the circulation via the paracellular route and form lipoprotein X (LpX) [31,32].

Hypercholesterolemia is almost always regarded as the major culprit for the development and progression of atherosclerosis. However, atherogenesis of hypercholesterolemia in patients with cholestatic disorders, such as primary biliary cirrhosis, remains a controversial subject [5–7]. Nagasaka et al. reported that the intimal–medial thickness of the cervical artery and the water stiffness in AGS children exhibiting profound hypercholesterolemia together with mild or less hyperbilirubinemia were similar to those in healthy age-matched children [6]. They postulated that a considerable increase in HDL may prevent the development of atherosclerosis. Nevertheless, considerable liver damage causing suppressed HDL together with moderate or more hyperbilirubinemia as was seen in our patients may engender atherosclerosis [1,6]. In this context, the establishment and achievement of optimal plasma lipoprotein levels are necessary.

In this study, we performed comprehensive analyses for expressions of genes involved in liver cholesterol regulation in AGS. However, the obtained information is still limited. Quantitative and functional analyses for proteins/enzymes encoded by each gene examined in this study will give us a better understanding of the liver cholesterol metabolism in AGS.

In conclusion, the results of this study in children with AGS suggested that the negative feedback loop mediated by SREBP2 expression

and maturation was impaired, and the major regulators of liver cholesterol, including *HMGCR*, *LDLR*, and *SR-BI*, were considerably upregulated, resulting in accelerated liver cholesterol accumulation.

Appendix A. Supplementary data

Supplementary data to this article can be found online at http://dx.doi.org/10.1016/j.cca.2014.10.034.

References

[1] Davit-Spraul A, Pourci ML, Atger V, et al. Abnormal lipoprotein pattern in patients with Alagille syndrome depends on Icterus severity. Gastroenterology 1996;111:1023–32.
[2] Hiraoka H, Yamashita S, Matsuzawa Y, et al. Decrease of hepatic triglyceride lipase levels and increase of cholesteryl ester transfer protein levels in patients with primary biliary cirrhosis: relationship to abnormalities in high-density lipoprotein. Hepatology 1993;18:103–10.
[3] Nagasaka H, Miida T, Hirano K, et al. Fluctuation of lipoprotein metabolism linked with bile acid-activated liver nuclear receptors in Alagille syndrome. Atherosclerosis 2008;198:434–40.
[4] McIntyre N, Harry DS, Pearson AJ. The hypercholesterolaemia of obstructive jaundice. Gut 1975;16:379–91.
[5] Van Dam GM, Gips CH. Primary biliary cirrhosis in The Netherlands. An analysis of associated diseases, cardiovascular risk, and malignancies on the basis of mortality figures. Scand J Gastroenterol 1997;32:77–83.
[6] Nagasaka H, Yorifuji T, Egawa H, et al. Evaluation of risk for atherosclerosis in Alagille syndrome and progressive familial intrahepatic cholestasis: two congenital cholestatic diseases with different lipoprotein metabolisms. J Pediatr 2005;146:329–35.
[7] Sorokin A, Brown JL, Thompson PD. Primary biliary cirrhosis, hyperlipidemia, and atherosclerotic risk: a systematic review. Atherosclerosis 2007;194:293–9.
[8] Oda T, Elkahloun AG, Pike BL, et al. Mutations in the human Jagged1 gene are responsible for Alagille syndrome. Nat Genet 1997;16:235–42.
[9] Li L, Krantz ID, Deng Y, et al. Alagille syndrome is caused by mutations in human Jagged1, which encodes a ligand for Notch1. Nat Genet 1997;16:243–51.
[10] Flynn DM, Nijjar S, Hubscher SG, et al. The role of Notch receptor expression in bile duct development and disease. J Pathol 2004;204:55–64.
[11] Emerick KM, Rand EB, Goldmuntz E, Krantz ID, Spinner NB, Piccoli DA. Features of Alagille syndrome in 92 patients: frequency and relation to prognosis. Hepatology 1999;29:822–9.
[12] Subramaniam P, Knisely A, Portmann B, et al. Diagnosis of Alagille syndrome-25 years of experience at King's College Hospital. J Pediatr Gastroenterol Nutr 2011;52:84–9.
[13] Kamath BM, Spinner NB, Emerick KM, et al. Vascular anomalies in Alagille syndrome: a significant cause of morbidity and mortality. Circulation 2004;109:1354–8.
[14] Gottrand F, Clavey V, Fruchart JC, Farriaux JP. Lipoprotein pattern and plasma lecithin cholesterol acyl transferase activity in children with Alagille syndrome. Atherosclerosis 1995;115:233–41.
[15] Lykavieris P, Hadchouel M, Chardot C, Bernard O. Outcome of liver disease in children with Alagille syndrome: a study of 163 patients. Gut 2001;49:431–5.
[16] Halilbasic E, Claudel T, Trauner M. Bile acid transporters and regulatory nuclear receptors in the liver and beyond. J Hepatol 2013;58:155–68.
[17] Loren J, Huang Z, Laffitte BA, Molteni V. Liver X receptor modulators: a review of recently patented compounds (2009–2012). Expert Opin Ther Pat 2013;23:1317–35.
[18] Chiang JY. Bile acids: regulation of synthesis. J Lipid Res 2009;50:1955–66.
[19] Malerod L, Sporstol M, Juvet LK, et al. Bile acids reduce SR-BI expression in hepatocytes by a pathway involving FXR/RXR, SHP, and LRH-1. Biochem Biophys Res Commun 2005;336:1096–105.
[20] Brown MS, Goldstein JL. The SREBP pathway: regulation of cholesterol metabolism by proteolysis of a membrane-bound transcription factor. Cell 1997;89:331–40.
[21] Eberle D, Hegarty B, Bossard P, Ferre P, Foufelle F. SREBP transcription factors: master regulators of lipid homeostasis. Biochimie 2004;86:839–48.
[22] McPherson R, Gauthier A. Molecular regulation of SREBP function: the Insig-SCAP connection and isoform-specific modulation of lipid synthesis. Biochem Cell Biol 2004;82:201–11.
[23] Folch J, Lees M, Sloane Stanley GH. A simple method for the isolation and purification of total lipides from animal tissues. J Biol Chem 1957;226:497–509.
[24] Beher WT, Stradnieks S, Lin GJ, Sanfield J. Rapid analysis of human fecal bile acids. Steroids 1981;38:281–95.
[25] Schmidt RJ, Ficorilli JV, Zhang Y, et al. A 15-ketosterol is a liver X receptor ligand that suppresses sterol-responsive element binding protein-2 activity. J Lipid Res 2006;47:1037–44.
[26] Davis RA, Miyake JH, Hui TY, Spann NJ. Regulation of cholesterol-7alpha-hydroxylase: BAREly missing a SHP. J Lipid Res 2002;43:533–43.
[27] Chen W, Owsley E, Yang Y, Stroup D, Chiang JY. Nuclear receptor-mediated repression of human cholesterol 7alpha-hydroxylase gene transcription by bile acids. J Lipid Res 2001;42:1402–12.
[28] Bilz S, Samuel V, Morino K, Savage D, Choi CS, Shulman GI. Activation of the farnesoid X receptor improves lipid metabolism in combined hyperlipidemic hamsters. Am J Physiol Endocrinol Metab 2006;290:E716–22.
[29] Enjoji M, Yada R, Fujino T, et al. The state of cholesterol metabolism in the liver of patients with primary biliary cirrhosis: the role of MDR3 expression. Hepatol Int 2009;3:490–6.
[30] Barak AJ, Sorrell MF, Tuma DJ. Effect of serum lipoproteins of bile obstructed rats on 3-hydroxy-3-methylglutaryl coenzyme A reductase activity in perfused rat liver. Lipids 1979;14:883–7.
[31] Bravo I, Amigo L, Cohen DE, et al. Role of plasma and liver cholesterol- and lipoprotein-metabolism determinants in LpX formation in the mouse. Biochim Biophys Acta 2007;1770:979–88.
[32] Elferink RP, Ottenhoff R, van Marle J, et al. P-glycoproteins mediate the formation of lipoprotein X in the mouse. J Clin Invest 1998;102:1749–57.

Research Article

EASL EUROPEAN ASSOCIATION FOR THE STUDY OF THE LIVER | JOURNAL OF HEPATOLOGY

Long-term native liver fibrosis in biliary atresia: Development of a novel scoring system using histology and standard liver tests

Hirofumi Tomita[1], Yohei Masugi[2], Ken Hoshino[1], Yasushi Fuchimoto[3], Akihiro Fujino[1], Naoki Shimojima[1], Hirotoshi Ebinuma[4], Hidetsugu Saito[4], Michiie Sakamoto[2], Tatsuo Kuroda[1,*]

[1]*Department of Pediatric Surgery, Keio University School of Medicine, 35 Shinanomachi, Shinjuku-ku, Tokyo 160-8582, Japan;* [2]*Department of Pathology, Keio University School of Medicine, 35 Shinanomachi, Shinjuku-ku, Tokyo 160-8582, Japan;* [3]*Division of Surgery, Department of Surgical Subspecialities, National Center for Child Health and Development, 2-10-1 Okura, Setagaya-ku, Tokyo 157-8535, Japan;* [4]*Department of Internal Medicine, Keio University School of Medicine, 35 Shinanomachi, Shinjuku-ku, Tokyo 160-8582, Japan*

Background & Aims: Although liver fibrosis is an important predictor of outcomes for biliary atresia (BA), postsurgical native liver histology has not been well reported. Here, we retrospectively evaluated postsurgical native liver histology, and developed and assessed a novel scoring system – the BA liver fibrosis (BALF) score for non-invasively predicting liver fibrosis grades.

Methods: We identified 259 native liver specimens from 91 BA patients. Of these, 180 specimens, obtained from 62 patients aged ⩾1 year at examination, were used to develop the BALF scoring system. The BALF score equation was determined according to the prediction of histological fibrosis grades by multivariate ordered logistic regression analysis. The diagnostic powers of the BALF score and several non-invasive markers were assessed by area under the receiver operating characteristic curve (AUROC) analyses.

Results: Natural logarithms of the serum total bilirubin, γ-glutamyltransferase, and albumin levels, and age were selected as significantly independent variables for the BALF score equation. The BALF score had a good diagnostic power (AUROCs = 0.86–0.94, p <0.001) and good diagnostic accuracy (79.4–93.3%) for each fibrosis grade. The BALF score revealed a strong correlation with fibrosis grade (r = 0.77, p <0.001), and was the preferable non-invasive marker for diagnosing fibrosis grades ⩾F2. In a serial liver histology subgroup analysis, 7/15 patients exhibited liver fibrosis improvement with BALF scores being equivalent to histological fibrosis grades of F0–1.

Conclusions: In postsurgical BA patients aged ⩾1 year, the BALF score is a potential non-invasive marker of native liver fibrosis.

Keywords: Biliary atresia; Hepatoportoenterostomy; Liver fibrosis; Liver biopsy; Non-invasive fibrosis marker.

Received 26 September 2013; received in revised form 18 December 2013; accepted 27 January 2014; available online 15 February 2014

* Corresponding author. Tel.: +81 3 5363 3024; fax: +81 3 3356 8804.

E-mail address: kuroda-t@z8.keio.jp (T. Kuroda).

Abbreviations: BA, biliary atresia; LT, liver transplantation; LDLT, living donor liver transplantation; BALF, biliary atresia liver fibrosis; PELD, pediatric end-stage liver disease; TB, total bilirubin; AST, aspartate aminotransferase; ALT, alanine aminotransferase; GGT, γ-glutamyltransferase; ChE, cholinesterase; PT-INR, prothrombin time-international normalized ratio; APRI, aspartate aminotransferase to platelet ratio index; PIIINP, procollagen type III amino-terminal peptide; AUROC, area under the receiver operating characteristic curve.

Introduction

Biliary atresia (BA) is a destructive, inflammatory, obliterative cholangiopathy that develops in 1/5,000 to 1/19,000 newborns [1]. The disease affects varying lengths of both the extra- and intra-hepatic bile ducts, and is classified according to the level of the most proximal part of the extra-hepatic biliary obstruction: atresia of the common bile duct (type 1), hepatic duct (type 2), or porta hepatis (type 3) [1,2]. To establish initial bile drainage, an anastomosis between the bile duct and the gastrointestinal tract can be created in certain cases ("correctable" BA, mostly type 1), but hepatoportoenterostomy is more often performed ("non-correctable" BA, mostly type 3) in such cases [2].

Hepatoportoenterostomy, first described by Kasai [3], can achieve initial bile drainage in 50–60% of cases [1]. However, liver fibrosis progresses rapidly before the bile drainage operation, and is an important predictor of outcome [4]. Even after successfully achieving bile drainage by portoenterostomy, progression of liver fibrosis may continue, leading to portal hypertension and cirrhosis [4]. Liver transplantation (LT) is performed when bile drainage is not achieved, or when complications of biliary cirrhosis occur [5]. Because of the progressive liver disease, long-term native liver survival is only achieved in approximately 20% of BA patients [4,5]. Thus, BA is the most common indication for LT in children; moreover, portoenterostomy is believed to be palliative, not curative [1].

Because of the severe shortage of organs from deceased donors in Japan [6], determination of the optimal time for living donor LT (LDLT) is important for BA patients. To investigate the postsurgical state of the native liver, we have performed percutaneous liver biopsies as part of the patient's routine follow-up. Because native liver fibrosis in postsurgical BA patients has not been well reported, we retrospectively analyzed the histology findings from 259 native liver specimens, and their associated

data, in 91 BA patients. From this, we developed a novel scoring system – the BA liver fibrosis (BALF) score – which is a non-invasive, practical, and easily accessible potential marker of liver fibrosis that is based on standard liver tests; its accuracy was also evaluated by comparing with the pediatric end-stage liver disease (PELD) score, which is widely used for liver allocation determinations [7], and the levels of several non-invasive fibrosis markers. Furthermore, we evaluated serial native liver histology in a subgroup of 15 patients.

Patients and methods

Study population and ethical considerations

We retrospectively identified 91 BA patients from whom native liver specimens had been obtained between March 1993 and February 2013 at Keio (Japan) University School of Medicine. The patients had either visited our institution for an initial operation, were referred to us for follow-up after an initial operation (42 patients), or had been referred to us due the presence of LT indicators (49 patients) after an initial operation for bile drainage. From the 91 patients, 259 liver specimens were collected by wedge biopsy during laparotomy (34 specimens), percutaneous needle biopsy (161 specimens), or were obtained from explanted livers during LT (64 specimens). From these specimens, we excluded 1 explanted liver because of a hepatitis C virus infection, and 18 specimens because of liver histology findings (described below).

Development of the BALF score was conducted from 180 histology examinations obtained from 62 patients aged ⩾1 year, because liver biochemistry results were likely elevated before surgery, and for a certain period after surgery, regardless of the liver fibrosis grade. Of the 180 specimens, the median number of specimens obtained from individual patients was 1 (range, 1–11). Of the 62 patients, 28 (45.2%) were male and 34 (54.8%) were female. Type 1 BA was diagnosed in 9 patients (14.5%), type 2 in 2 (3.2%), and type 3 in 45 (72.6%); the diagnosis was unknown in 6 (9.7%). The initial surgery for bile drainage was hepaticoenterostomy in 6 patients (9.7%), hepatoportoenterostomy in 54 (87.1%), and an unknown procedure in 2 (3.2%); the median age at the time of the initial surgery was 64 days (range, 17–151 days). Selection of the study population is summarized in Fig. 1. This study conformed to the ethical guidelines of the 1975 Declaration of Helsinki, and was approved by the ethical committee at Keio University School of Medicine (2012-173).

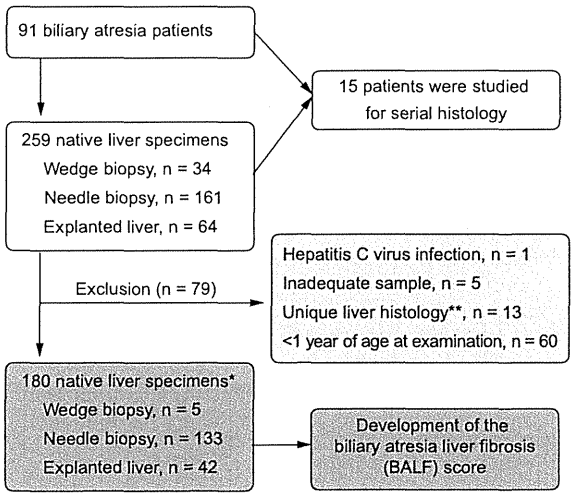

Fig. 1. Selection of the study population. *Obtained from 62 patients. **One patient revealed unique liver histology findings, indicating ductopenia, accompanied by little evidence of fibrosis in 13 serial percutaneous biopsies.

Data collection

The patients' clinical courses, documented pathological findings, and laboratory results around the time of liver specimen collection were collected from the patients' medical records. Collected standard biochemical test results included serum levels of total bilirubin (TB), aspartate aminotransferase (AST), alanine aminotransferase (ALT), γ-glutamyltransferase (GGT), albumin, and cholinesterase (ChE). Collected hematological test results included prothrombin time-international normalized ratios (PT-INR) and platelet counts. These standard biochemical and hematological test results were obtained for all corresponding histological examinations. The PELD score [7] was calculated using the following equation:

$$\text{PELD score} = \{0.463 \times (\text{age} < 1\,\text{year}^{*}) - 0.687 \times \text{Log}_e[\text{albumin (g/dl)}] + 0.480 \times \text{Log}_e[\text{TB (mg/dl)}] + 1.857 \times \text{Log}_e(\text{PT-INR}) + 0.667 \times (\text{growth failure} < -2\ \text{standard deviation}^{**})\} \times 10$$

*Age was coded as 1 for children under 1 year; in other cases, it was coded as 0.

**Growth failure was coded as 1 for children, with height or weight <−2 standard deviations below age-specific normal values; in other cases, it was coded as 0.

As a non-invasive fibrosis marker, the AST to platelet ratio index (APRI) [8] was also calculated; a serum AST level of 35 IU/L was used as the upper normal limit:

$$\text{APRI} = \{(\text{AST/upper normal limit})/[\text{platelet counts } (10^9/\text{L})]\} \times 100$$

The APRIs in patients having a history of splenectomy, partial splenic embolization, or with biliary atresia splenic malformation syndrome were excluded from further analyses. Direct serum fibrosis markers, including serum levels of hyaluronic acid, type IV collagen 7S domain, and procollagen type III amino-terminal peptide (PIIINP) [9], were collected for most of the corresponding histological examinations. The normal ranges are ⩽50.0 ng/ml for hyaluronic acid, ⩽6.0 ng/ml for type IV collagen 7S domain, and 0.30–0.80 U/ml for PIIINP.

Evaluation of liver histology

Wedge biopsy specimens, ⩾5 mm in size, were obtained by surgical resection from the edge of the liver during laparotomy. Percutaneous liver biopsies, ⩾1.0 cm in length, were performed with an 18-gauge suction needle under ultrasonographic guidance. All of the biopsies and operations were performed after obtaining written informed consent. The biopsy specimens and explanted livers were fixed in formalin, embedded in paraffin, sectioned, and stained with hematoxylin-eosin, Azan-Mallory, and Elastica van Gieson stains. Liver fibrosis was evaluated based on the documented pathological findings that had been reported at the time of examination by experienced pathologists, according to the METAVIR scoring system [10] or the new Inuyama classification [11] as follows: F0, no portal fibrosis; F1, portal fibrosis without septa; F2, portal fibrosis with rare septa; F3, numerous septa or lobular distortion without cirrhosis; and F4, cirrhosis. Five specimens, containing no or few portal tracts, were indeterminate for fibrosis grade. One patient revealed unique liver histology findings, indicating ductopenia, accompanied by little evidence of fibrosis in 13 serial percutaneous biopsies. When compared to the other subjects, the blood test results for this patient did not correspond to the histological fibrosis grade; therefore, these 13 specimens were excluded from the analysis.

Development of the BALF score by ordered logistic regression analysis

To predict the histological fibrosis grade, ordered logistic regression analyses were performed, using the histological fibrosis grades as ordinal data (F0, F1, F2, F3, and F4) for the dependent variable; the independent variables included logarithmic transformations of the collected standard biochemical and hematological test results, and age at the time of the corresponding histological examination. For multivariate logistic regression analysis, independent variables showing strong correlations ($|r| > 0.7$) to each other were avoided because of multicollinearity concerns. The equation comprising the BALF score was developed by adding a minus sign to the regression equation for the logit of F0 probability in the multivariate analysis.

Table 1. Baseline data, stratified by histological fibrosis grade, for the development of the biliary atresia liver fibrosis (BALF) score.

	F0 (n = 15)	F1 (n = 53)	F2 (n = 44)	F3 (n = 34)	F4 (n = 34)
TB (mg/dl)	0.5 (0.2-0.9)	0.7 (0.3-10.1)	0.8 (0.3-11.5)	1.9 (0.4-24.5)	7.2 (0.3-30.1)
AST (IU/L)	33 (25-83)	36 (18-550)	75 (22-251)	108 (35-1065)	181 (94-472)
ALT (IU/L)	22 (14-79)	35 (9-676)	64 (13-457)	86 (21-411)	133 (37-587)
GGT (IU/L)	44 (10-102)	68 (7-1108)	142 (8-1384)	204 (66-1456)	317 (32-1817)
Albumin (g/dl)	4.4 (3.7-4.7)	4.1 (3.1-5.1)	4.0 (3.0-5.1)	3.7 (2.4-4.6)	3.2 (1.5-4.5)
ChE (IU/L)	326 (220-598)	342 (97-567)	278 (122-581)	185 (46-335)	141 (43-323)
PT-INR	1.07 (1.00-1.21)	1.07 (0.91-1.47)	1.03 (0.86-1.25)	1.04 (0.86-2.01)	1.14 (0.89-1.48)
Platelet count (× 10^9/L)	141 (70-356)	165 (52-372)	127 (45-392)	113 (56-446)	152 (42-524)
Age (yr)	9.7 (1.1-18.8)	7.0 (1.2-19.9)	5.3 (1.2-19.2)	7.4 (1.1-25.4)	2.4 (1.0-33.6)

Data are presented as median (range).
TB, total bilirubin; AST, aspartate aminotransferase; ALT, alanine aminotransferase; GGT, γ-glutamyltransferase; ChE, cholinesterase; PT-INR, prothrombin time-international normalized ratio.

Assessment of the BALF score

After developing the BALF score equation, the score at the time of each histological examination was calculated. The BALF score and other non-invasive markers were assessed in the same population that was used for development of the BALF score equation. We also calculated and evaluated the BALF score results in patients aged <1 year before and after bile drainage surgery.

Analysis of serial liver histology and the BALF score in each patient

Among the 91 patients involved in this study, 31 underwent histological examinations at the time of their initial operation during the study period. Of these, 15 had repeated histological examinations when they were aged ⩾2 years and these patients were individually analyzed to obtain serial data. Among the other 16 patients, 4 underwent primary LDLT; 1 died suddenly at 11 months of age; 5 underwent LDLT before 2 years of age; 5 were <2 years of age at the time of this analysis; and 1 patient, who had undergone hepaticoenterostomy for type 2 BA, did not undergo a histological examination after reaching 2 years of age.

Statistical analysis

The categorical data are presented as frequencies (%), and the continuous data are presented as medians (ranges). Correlations between the ordinal and/or continuous data were assessed by Spearman's correlation coefficient (r). For logistic regression analyses, the *p* value of each independent variable was determined by the Wald chi-square value (Wald), which was calculated by squaring the ratio of the regression coefficient divided by its standard error. The diagnostic powers of the BALF score and the other fibrosis markers were assessed by area under the receiver operating characteristic curve (AUROC) analyses; an AUROC of 1.0 indicates a test of perfect diagnostic power, and that of 0.5 indicates a test without diagnostic power. The cut-off values were determined by maximizing the sum of the sensitivity and specificity on Youden's index [12]. *p* values <0.05 were considered statistically significant. Statistical analyses were performed using SPSS 20.0 software (IBM SPSS, Chicago, IL, USA).

Results

Development of the BALF score by ordered logistic regression analysis

Baseline data corresponding to the 180 histology examinations for the development of the BALF score, stratified by histological fibrosis grade, are summarized in Table 1; the results of the ordered logistic regression analyses are shown in Table 2. In the univariate analyses, natural logarithms of the serum TB levels provided the most significant coefficients (Wald = 89.240, $p < 0.001$). In the multivariate analysis, natural logarithms of the

Table 2. Ordered logistic regression analyses for liver fibrosis grades, F0–F4.

Variable	Coefficient (95% CI)	Standard error	Wald	*p* value
Univariate analysis				
Log_e [TB (mg/dl)]	1.854 (1.470-2.239)	0.196	89.240	<0.001
Log_e [AST (IU/L)]	1.926 (1.493-2.358)	0.221	76.107	<0.001
Log_e [ALT (IU/L)]	1.218 (0.886-1.550)	0.169	51.737	<0.001
Log_e [GGT (IU/L)]	0.858 (0.617-1.100)	0.123	48.448	<0.001
Log_e [albumin (g/dl)]	-8.017 (-10.139--5.896)	1.082	54.871	<0.001
Log_e [ChE (IU/L)]	-3.218 (-3.948--2.487)	0.373	74.527	<0.001
Log_e [PT-INR]	2.627 (0.342-4.913)	1.166	5.078	0.02
Log_e [platelet count (× 10^9/L)]	-0.299 (-0.799-0.202)	0.255	1.370	0.24
Log_e [age (years)]	-0.438 (-0.742--0.134)	0.155	7.994	0.005
Multivariate analysis				
Log_e [TB (mg/dl)]	1.438 (0.974-1.903)	0.237	36.861	<0.001
Log_e [GGT (IU/L)]	0.434 (0.159-0.710)	0.140	9.557	0.002
Log_e [albumin (g/dl)]	-3.491 (-5.805--1.177)	1.181	8.745	0.003
Log_e [age (years)]	-0.670 (-1.031--0.308)	0.184	13.196	<0.001

TB, total bilirubin; AST, aspartate aminotransferase; ALT, alanine aminotransferase; GGT, γ-glutamyltransferase; ChE, cholinesterase; PT-INR, prothrombin time-international normalized ratio.

Table 3. Diagnostic accuracy of the biliary atresia liver fibrosis (BALF) score in predicting histological fibrosis grade.

	AUROC	95% CI	Cut-off	Sensitivity	Specificity	Accuracy
≥F1	0.91*	0.86-0.96	1.96	77.6%	100%	79.4%
≥F2	0.86*	0.81-0.92	2.42	86.6%	73.5%	81.7%
≥F3	0.91*	0.87-0.95	4.12	83.8%	81.3%	82.2%
=F4	0.94*	0.90-0.99	5.64	94.1%	93.2%	93.3%

*p <0.001.
AUROC, area under the receiver operating characteristic curve.

serum TB, GGT, and albumin levels, and age at examination were selected as significant independent variables. Based on the multivariate analysis, the BALF score equation was developed:

$$\text{BALF score} = 7.196 + 1.438 \times \text{Log}_e[\text{TB (mg/dl)}] + 0.434 \times \text{Log}_e[\text{GGT (IU/L)}] - 3.491 \times \text{Log}_e[\text{albumin (g/dl)}] - 0.670 \times \text{Log}_e[\text{age (years)}]$$

Diagnostic accuracy of the BALF score

Table 3 shows the AUROC, cut-off value, and diagnostic accuracy of the BALF score for each fibrosis grade. The BALF score had good diagnostic power for predicting each fibrosis grade (AUROCs = 0.86–0.94, p <0.001), and the cut-off values were calculated as 1.96 for a fibrosis grade ⩾F1, 2.42 for ⩾F2, 4.12 for ⩾F3, and 5.64 for F4; the score provided good diagnostic accuracy in diagnosing each fibrosis grade (79.4–93.3%).

Comparisons of the BALF score, PELD score, and other non-invasive fibrosis markers

Fig. 2 shows the boxplots for the BALF score, PELD score, APRI, and levels of serum hyaluronic acid, type IV collagen 7S domain, and PIIINP *vs.* the histological fibrosis grade. Of these, the BALF score was most strongly correlated with the histological fibrosis grade (r = 0.77, p <0.001). The BALF score was equally distributed from F0 to F4. The diagnostic powers of the BALF score and the other markers for diagnosing fibrosis grades ⩾F2 and F4, assessed by AUROC analyses, are shown in Fig. 3. For diagnosing fibrosis grades ⩾F2, the BALF score had the highest diagnostic power (AUROC = 0.86, p <0.001), followed by the PELD score and the APRI (AUROC = 0.80, p <0.001), but the direct serum markers showed relatively low or no significant diagnostic power. The PELD score, hyaluronic acid levels, and type IV collagen 7S domain levels, as well as the BALF score, showed excellent diagnostic powers for diagnosing an F4 fibrosis grade (AUROC >0.90, p <0.001).

Changes in the BALF score before and after bile drainage surgery

The BALF scores for patients aged <1 year, before and after initial surgery (n = 31 and n = 29, respectively), compared to patients aged 1–2 years, after surgery (n = 28), are shown in Fig. 4. The BALF scores were apparently high before surgery, regardless of the fibrosis grades. Even after bile drainage surgery, patients aged <1 year showed high score values. The BALF scores in the patients aged 1–2 years were comparable with those for all patients aged ⩾1 year.

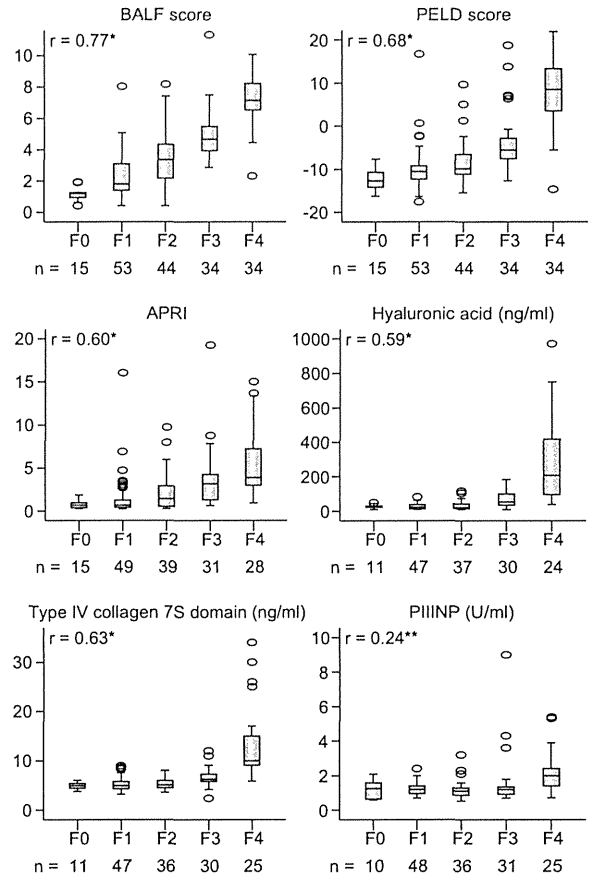

Fig. 2. Comparisons of the biliary atresia liver fibrosis (BALF) score, the pediatric end-stage liver disease (PELD) score, and several non-invasive fibrosis markers. Boxplots show the median values with the interquartile ranges, and error bars indicate the smallest and the largest values within 1.5 box-lengths of the upper and the lower quartiles. Outliers represent the individual points by circles. Correlations between the scores/markers and the histological fibrosis grades were evaluated by Spearman's correlation coefficient (r); *p <0.001, **p = 0.009. APRI, aspartate aminotransferase to platelet ratio index; PIIINP, procollagen type III amino-terminal peptide.

Serial liver histology and BALF score in each patient

The status of the initial operations and the most recent histological examinations for 15 patients are shown in Table 4. Cases 1–7 showed some liver fibrosis relief with BALF scores being equivalent to F0–1; these 7 patients achieved good physical growth and

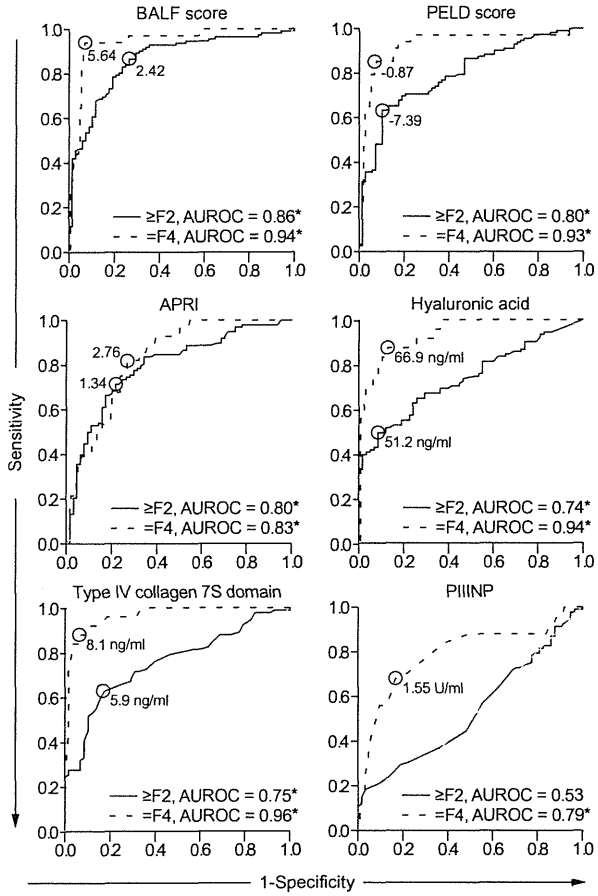

Fig. 3. The diagnostic powers of the biliary atresia liver fibrosis (BALF) score, pediatric end-stage liver disease (PELD) score, and non-invasive markers for liver fibrosis. The diagnostic power of each score/marker was assessed by calculating the area under the receiver operating characteristic curve (AUROC); solid lines, for diagnosing ≥F2; dashed lines, for diagnosing F4; gray lines, reference lines; circles, cut-off points (with cut-off values); *p <0.001. APRI, aspartate aminotransferase to platelet ratio index; PIIINP, procollagen type III amino-terminal peptide.

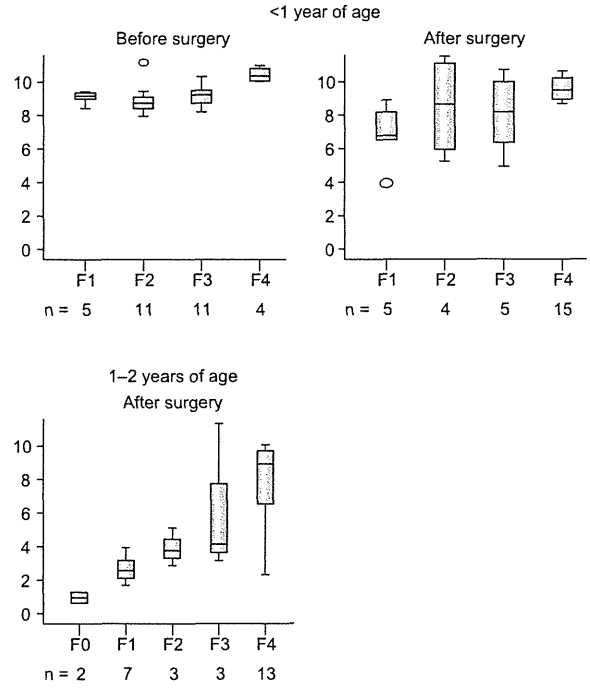

Fig. 4. Changes in the BALF score, before and after bile drainage surgery. Boxplots show the median values with the interquartile ranges, and error bars indicate the smallest and the largest values within 1.5 box-lengths of the upper and the lower quartiles. Outliers represent the individual points by circles.

social activity. Cases 8–12 showed the same grade of fibrosis in the initial and latest histological examinations; 3 of them had shown initial transient relief of liver fibrosis followed by worsening fibrosis, associated with repetitive cholangitis (Cases 10 and 11) or hepatopulmonary syndrome (Case 12). Cases 13–15 showed worsening liver fibrosis and relatively high BALF scores. Only Case 12 underwent LT during the study period; Cases 13–15 seemed likely to require LT in the near future due the presence of severe portal hypertension.

Discussion

Although hepatoportoenterostomy can achieve complete jaundice resolution in up to 60% of children with BA, liver fibrosis – a prominent feature of BA – may continue to progress [1,4,5]. Although LT in children with failed bile drainage surgery is certain, the timing of LT after successful bile drainage is debatable [13]. In Japan, grafts for LT rely almost entirely on living donors, especially from the parents of affected children [6]. Due to the increasing parental age and the required graft volume against the physical growth of the recipients, LDLT may not be possible, in some cases. Moreover, one large Japanese study indicated poor outcomes of adult-to-adult LDLT for postoperative BA patients, and the authors encouraged proactive consideration of LDLT at the earliest possible stage [14]. At our institution, hepatoportoenterostomy and LT for BA patients have been performed by the same team since the introduction of LDLT in 1995. To assess the native liver status more precisely, we introduced liver biopsies as the gold standard method for assessing liver fibrosis, with endoscopic screening of postsurgical BA patients. At first, liver fibrosis was supposed to progress in most BA patients, suggesting the future need for LT; only stable disease was believed to provide the patients and their parents with some relief. Thereafter, we noticed that certain patients demonstrated fibrosis improvement. Concerns about biopsy sampling errors were alleviated by serial liver histology, thus providing more substantial relief.

The BALF regression equation suggests that long-term native liver fibrosis in BA is influenced by the patient's bile drainage status, represented by the levels of serum TB and GGT. Some patients, especially older children or adults, develop decreasing liver synthetic capacity despite relatively small elevations in serum TB levels (data not shown). Thus, serum albumin levels represent a significant negative coefficient in the multivariate ordered logistic regression analysis. Additionally, the age at examination also showed a significant negative coefficient, suggesting that liver fibrosis could be improved over time, even in

Table 4. The status of 15 patients individually examined by serial liver histology.

Case No.	Disease type	Initial operation			Recent histological examination		
		Age (days)	Procedure	Fibrosis grade	Age (years)	Fibrosis grade	BALF score
1	Type 1	17	Hepaticoenterostomy	F2	2.5	F0	1.26
2	Type 1	24	Hepaticoenterostomy	F3	12.5	F1	1.17
3	Type 1	31	Portoenterostomy	F2	6.4	F1	1.50
4	Type 1	55	Portoenterostomy	F2	11.0	F0	1.26
5	Type 3	78	Portoenterostomy	F3	3.3	F1	2.12
6	Type 3	74	Portoenterostomy	F3	18.3	F1	0.84
7	Type 3	74	Portoenterostomy	F2	18.8	F0	1.19
8	Type 3	47	Portoenterostomy	F2	7.1	F2	2.44
9	Type 3	47	Portoenterostomy	F1	14.8	F1	2.34
10	Type 3	105	Portoenterostomy	F2	7.8	F2	2.20
11	Type 3	51	Portoenterostomy	F3	8.1	F3	3.24
12	Type 3	105	Portoenterostomy	F3	9.3	F3	4.84
13	Type 3	56	Portoenterostomy	F1	9.3	F2	3.94
14	Type 3	56	Portoenterostomy	F1	7.1	F3	4.68
15	Type 3	57	Portoenterostomy	F2	3.5	F3	6.26

BALF, biliary atresia liver fibrosis.

BA patients. Recently, liver fibrosis has been indicated to be reversible in a number of liver diseases, but data for BA are limited [4]. A few serial liver histology reports from the 1960s to 1980s documented fibrosis relief in some cases [15–18]. Thereafter, only a few studies have involved postsurgical liver histology [19,20]; however, serial data have not been presented. In a subpopulation of the current study, 7 of the 15 patients who achieved long-term native liver survival revealed some liver fibrosis relief during the study period.

The BALF score is the first non-invasive fibrosis marker developed for postsurgical BA patients based on liver histology findings, including the findings of percutaneous needle biopsy examinations obtained from patients with good postoperative courses. However, the PELD score was developed based on poor outcomes, such as patient death or movement to an intensive care unit, in children awaiting LT [7,21]. Although the BALF and PELD scores share the same independent variables (natural logarithms of serum TB and albumin levels), the BALF score results were more spread out than the PELD score results in the low fibrosis grade groups (F0–F3); moreover, the PELD score results were more spread out among the patients with cirrhosis (F4) than were the BALF score results (Fig. 1). Thus, the BALF score appears to be suitable for all patients (F0–4), but the PELD score seems best suited for severely affected patients, such as those with cirrhosis (F4), reflecting the methods used for the development of each score. The APRI consists of only two variables, is much simpler to calculate, and has been investigated in relation to prognosis [22], portal venous pressure [23], and fibrosis grade [24] at the time of Kasai hepatoportoenterostomy. Moreover, the APRI was used as a surrogate fibrosis marker in a prospective study examining steroid therapy in BA patients [25].

Although the current study contains one of the largest series of native liver histologies reported for BA patients, several limitations remain. First, the current study used liver histology findings, obtained from liver biopsies or explanted liver examinations, as reference parameters. Since biopsies are limited by sampling errors [26] and observer variability [27], the histological results are subject to omissions and false-positive results. In addition, segmental bile drainage, often observed in postsurgical BA patients [28] or small biopsy samples, may have resulted in an increased level of sampling error [26]. Second, this study had a relatively small sample size and a heterogeneous study population. Not all of the patients were evaluated by serial liver histology, after surgery, and the number of examinations in the same patient also differed; we analyzed the data from the same patient as independent data. We could not provide a validation group for the newly developed BALF scoring system because of the small and heterogeneous study population.

In the present study, we developed a potential fibrosis marker for postsurgical BA patients that is non-invasive, practical, and easily accessible. Because of a lack of validation, the BALF score should be further investigated with regard to its relationship with several parameters, such as long-term outcomes, postsurgical complications, and liver fibrosis. However, we believe that the BALF score will be a useful surrogate fibrosis marker in a future interventional trial.

Financial support

This study was supported by a grant from The Ministry of Health, Labour and Welfare of Japan (H24-Nanchi-Ippan-037, Health Labour Sciences Research Grants for Research on intractable diseases).

Conflict of interest

The authors who have taken part in this study declared that they do not have anything to disclose regarding funding or conflict of interest with respect to this manuscript.

References

[1] Hartley JL, Davenport M, Kelly DA. Biliary atresia. Lancet 2009;374:1704–1713.
[2] Nio M, Ohi R. Biliary atresia. Semin Pediatr Surg 2000;9:177–186.

[3] Kasai M, Suzuki S. A new operation for "noncorrectable" biliary atresia; hepatic portoenterostomy. Shujutsu (Operation) 1959;13:733–739, [In Japanese].
[4] Haafiz AB. Liver fibrosis in biliary atresia. Expert Rev Gastroenterol Hepatol 2010;4:335–343.
[5] Lykavieris P, Chardot C, Sokhn M, Gauthier F, Valayer J, Bernard O. Outcome in adulthood of biliary atresia: a study of 63 patients who survived for over 20 years with their native liver. Hepatology 2005;41:366–371.
[6] Tanabe M, Kawachi S, Obara H, Shinoda M, Hibi T, Kitagawa Y, et al. Current progress in ABO-incompatible liver transplantation. Eur J Clin Invest 2010;40:943–949.
[7] Freeman Jr RB, Wiesner RH, Harper A, McDiarmid SV, Lake J, Edwards E, et al. The new liver allocation system: moving toward evidence-based transplantation policy. Liver Transpl 2002;8:851–858.
[8] Wai CT, Greenson JK, Fontana RJ, Kalbfleisch JD, Marrero JA, Conjeevaram HS, et al. A simple non-invasive index can predict both significant fibrosis and cirrhosis in patients with chronic hepatitis C. Hepatology 2003;38:518–526.
[9] Gressner OA, Weiskirchen R, Gressner AM. Biomarkers of liver fibrosis: clinical translation of molecular pathogenesis or based on liver-dependent malfunction tests. Clin Chim Acta 2007;381:107–113.
[10] Bedossa P, Poynard T. An algorithm for the grading of activity in chronic hepatitis C. The METAVIR Cooperative Study Group. Hepatology 1996;24:289–293.
[11] Ichida F, Tsuji T, Omata M, Ichida T, Inoue K, Kamimura T, et al. New Inuyama classification; new criteria for histological assessment of chronic hepatitis. Int Hepatol Commun 1996;6:112–119.
[12] Youden WJ. Index for rating diagnostic tests. Cancer 1950;3:32–35.
[13] Kyoden Y, Tamura S, Sugawara Y, Yamashiki N, Matsui Y, Togashi J, et al. Outcome of living donor liver transplantation for post-Kasai biliary atresia in adults. Liver Transpl 2008;14:186–192.
[14] Uchida Y, Kasahara M, Egawa H, Takada Y, Ogawa K, Ogura Y, et al. Long-term outcome of adult-to-adult living donor liver transplantation for post-Kasai biliary atresia. Am J Transplant 2006;6:2443–2448.
[15] Bunton GL, Cameron R. Regeneration of liver after biliary cirrhosis. Ann N Y Acad Sci 1963;111:412–421.
[16] Altman RP, Chandra R, Lilly JR. Ongoing cirrhosis after successful portico-enterostomy in infants with biliary atresia. J Pediatr Surg 1975;10:685–691.
[17] Kasai M, Watanabe I, Ohi R. Follow-up studies of long term survivors after hepatic portoenterostomy for "noncorrectable" biliary atresia. J Pediatr Surg 1975;10:173–182.
[18] Gautier M, Valayer J, Odievre M, Alagille D. Histological liver evaluation 5 years after surgery for extrahepatic biliary atresia: a study of 20 cases. J Pediatr Surg 1984;19:263–268.
[19] Hasegawa T, Sasaki T, Kimura T, Hoki M, Okada A, Mushiake S, et al. Measurement of serum hyaluronic acid as a sensitive marker of liver fibrosis in biliary atresia. J Pediatr Surg 2000;35:1643–1646.
[20] Hadzic N, Davenport M, Tizzard S, Singer J, Howard ER, Mieli-Vergani G. Long-term survival following Kasai portoenterostomy: is chronic liver disease inevitable? J Pediatr Gastroenterol Nutr 2003;37:430–433.
[21] McDiarmid SV, Anand R, Lindblad AS. Principal Investigators and Institutions of the Studies of Pediatric Liver Transplantation Research Group. Development of a pediatric end-stage liver disease score to predict poor outcome in children awaiting liver transplantation. Transplantation 2002;74:173–181.
[22] Grieve A, Makin E, Davenport M. Aspartate Aminotransferase-to-Platelet ratio index (APRi) in infants with biliary atresia: prognostic value at presentation. J Pediatr Surg 2013;48:789–795.
[23] Shalaby A, Makin E, Davenport M. Portal venous pressure in biliary atresia. J Pediatr Surg 2012;47:363–366.
[24] Kim SY, Seok JY, Han SJ, Koh H. Assessment of liver fibrosis and cirrhosis by aspartate aminotransferase-to-platelet ratio index in children with biliary atresia. J Pediatr Gastroenterol Nutr 2010;51:198–202.
[25] Davenport M, Parsons C, Tizzard S, Hadzic N. Steroids in biliary atresia: Single surgeon, single centre, prospective study. J Hepatol 2013;59:1054–1058.
[26] Bedossa P, Dargere D, Paradis V. Sampling variability of liver fibrosis in chronic hepatitis C. Hepatology 2003;38:1449–1457.
[27] Bedossa P. The French METAVIR Cooperative Study Group. Intraobserver and interobserver variations in liver biopsy interpretation in patients with chronic hepatitis C. Hepatology 1994;20:15–20.
[28] Takahashi A, Masuda N, Suzuki M, Shimura T, Nomoto K, Suzuki N, et al. Evidence for segmental bile drainage by hepatic portoenterostomy for biliary atresia: cholangiographic, hepatic venographic, and histologic evaluation of the liver taken at liver transplantation. J Pediatr Surg 2004;39:1–5.

II. 疾患各論：消化器疾患

ウイルス性肝炎，その他の慢性肝疾患

KeyWords
◎ウイルス性慢性肝炎
◎糖原病
◎Wilson病
◎シトリン欠損症
◎発がん

Author 乾(いぬい)あやの*，角田(つのだ)知之(ともゆき)*，川本愛理(かわもとまなり)*

*済生会横浜市東部病院　小児肝臓消化器科

Headline

1. 小児期発症の慢性肝疾患は，症状に乏しく患児の病識が薄いことが多い．
2. 長期予後が著しく改善したため，成人期での新たな合併症の出現が今後の課題である．
3. 成人期の肝がん発生の危険性を認識する．

はじめに

小児期の慢性肝疾患は多岐にわたる．他の小児期発症の慢性疾患と同様に疾患が重篤で病悩期が長いほど患家は依存心が強く，かつ自立心が弱い．したがって，これを克服するのが内科医にトランジションする絶好の時期と考えられる．本稿では，おもに頻度の高い代謝性肝疾患を中心に述べる．

小児期の肝疾患における検査値の特徴

1．胆汁うっ滞

成人では，アルコール性肝疾患などでγ-GTPが上昇するため，胆汁うっ滞の指標にはALPを用いる．しかし，小児期は骨の成長期であり，ALPはしばしば高値を呈する．トランスアミナーゼが正常でALPのみが高値の場合，アイソザイムを測定するとそのほとんどが骨型である．逆に，小児期はアルコールや食事によるγ-GTPへの影響はほとんどない．したがって，小児期の胆汁うっ滞の評価はγ-GTPで行っている．

2．線維化

成人では，線維化のマーカーとしてヒアルロン酸，IV型コラーゲン，P-III-Pが指標として用いられる．しかし，これらのマーカーは小児期では他の疾患でもしばしば高値となり，指標としては不適当である．線維化あるいは肝硬変に最もよい指標は血小板数である．

慢性肝疾患各論

1．ウイルス性慢性肝炎

内科医にトランジションするにあたって，ウイルス性慢性肝炎については，日本肝臓学会のホームページに掲載されているB型肝炎診療ガイドラインならびにC型肝炎診療ガイドラインに則って診療するのが適切である．その際，小児科医としては日本肝臓学会専門医に紹介することが重要である．

小児期のウイルス性慢性肝炎患者のなかで注意が必要なのは，小児期から心疾患や血液悪性腫瘍などの基礎疾患があり輸血関連でウイルス性慢性肝炎を合併した場合である．これらの疾患については，本特集の他稿を参照していただきたいが，小児肝臓専門医からみると基礎疾患がない患児に比して，患家は医師に対して依存度が高く，自立心も弱い．

2．肝型糖原病

肝型糖原病は，代謝を担う酵素活性低下によって肝内に正常あるいは異常な形態のグリコーゲンが蓄積する遺伝性疾患である．肝型

0370-999X/13/¥100/頁/JCOPY